Aus dem Institut für Humangenetik

(Prof. Dr. med. B. Wollnik)

der Medizinischen Fakultät der Universität Göttingen

The role of Hedgehog signaling and its interaction with EGFR-pathway in cutaneous squamous cell carcinoma

INAUGURAL-DISSERTATION

zur Erlangung des Doktorgrades

der Medizinischen Fakultät der

Georg-August-Universität zu Göttingen

vorgelegt von

Natalia Khizanishvili

aus

Tbilisi, Georgien

Göttingen 2019

Dekan:	Prof. Dr. med. W. Brück

Betreuungsausschuss

Betreuer/in	Prof. Dr. med. H. Hahn
Ko-Betreuer/in:	Prof. Dr. med. M. Schön

Prüfungskommission

Referent/in	Prof. Dr. med. H. Hahn
Ko-Referent/in:	Prof. Dr. hum. biol. M. Schön
Drittreferent/in:	Prof. Dr. mult. T. Meyer

Datum der mündlichen Prüfung: 06.08.2020

Dedicated to my dear father Levan Khizanishvili

ვუძღვნი ძვირფას მამას - ლევან ხიზანიშვილს

Parts of this work have been published:

Pyczek J, **Khizanishvili N**, Kuzyakova M, Zabel S, Bauer J, Nitzki F, Emmert S, Schön MP, Boukamp P, Schildhaus H-U, Uhmann A and Hahn H (2019): Regulation and Role of GLI1 in Cutaneous Squamous Cell Carcinoma Pathogenesis. Front. Genet. 10:1185. doi: 10.3389/fgene.2019.01185

Table of Contents

List of Figures

List of Tables

Abbreviations

AK	actinic keratosis
AKT	v-akt murine thymoma viral oncogene homolog
ATO	arsenic trioxide
ATP	adenosine triphosphate
BCA	bicinchoninic acid
BCC	basal cell carcinoma
BrdU	5-bromo-2-deoxyuridine
BSA	bovine serum albumin
BTC	betacellulin
CDH	E-cadherine
cDNA	copyDNA
Cos2	kinesin-related protein costal2
cSCC	cutaneous squamous cell carcinoma
Dhh	desert hedgehog
Disp	dispatched
DMEM	Dulbecco's Modified Eagle Medium
DNA	deoxyribonucleic acid
DNase	deoxyribonuclease
dNTP	deoxyribonucleotide triphosphate
DTT	dithiothreitol
EDTA	ethylenediaminetetraacetic acid
EGF	epidermal growth factor
EGFR	epidermal growth factor receptor
EMT	epithelial to mesenchymal transition
EPR	epiregulin

ERAD	ER-associated degradation
ERK	extracellular signal-regulated kinases
EtOH	ethanol
FCS	fetal calf serum
FDA	Food and Drug Administration
FZD	frizzled
GLI/Gli	glioma-associated oncogene
GLI_{act}	GLI activator form
GLI_{rep}	GLI repressor form
GTP	guanosine triphosphate
GTPase	guanosine triphosphate hydrolase
HH	hedgehog
HhA	HH antagonist
HHIP	hedgehog interacting protein
HNSCC	head and neck squamous cell carcinoma
HPRT	hypoxanthine-guanine phosphoribosyl transferase
HPV	human papillomavirus
HRP	horseradish peroxidase
HSC70	heat shock protein 70
IHH	indian hedgehog
IL-1ß	interleukin-1ß
LEF	lymphoid enhancer factor
LOH	loss of heterozygosity
MB	medulloblastoma
MEK/MAPK	mitogen-activated protein kinase kinase
MMS	Mohs micrographic surgery
mRNA	messenger ribonucleic acid

mTOR	mammalian target of rapamycin
Myc	myelocytomatosis oncogene
NEAA	non-essential amino acids
NFκB	nuclear factor kappa-light-chain-enhancer of activated B cells
NMSC	non-melanoma skin cancer
NSCLC	non-small cell lung cancer
NTC	no-template-control
OTRs	organ transplant recipients
P/S	penicillin streptomycin
PBS	phosphate-buffered saline
PBS-T	phosphate-buffered saline - tween 20
pDNA	plasmidDNA
PI3K	phosphatidylinositol-4,5-biphosphate-3-kinase
PTCH /Ptch	patched
PUVA	psoralen and UV-A
qRT-PCR	quantitative real time polymerase chain reaction
Rac1	ras-related C3 botulinum toxin substrate 1
Raf	rapidly accelerated fibrosarcoma
RAS	rat sarcoma
RhoA	ras homolog family member A
RNase	ribonuclease
RT	room temperature
RTK	receptor tyrosine kinases
SAG	smoothened agonist
SANT1	synthetic smoothened antagonist 1
SDS	sodiumdodecylsulfate
Ser	serine

SHH/Shh	sonic hedgehog
siRNA	small interfering RNA
SMO/Smo	smoothened
SOS	son of sevenless
SUFU/SuFu	suppressor of fused
TGF-β	transforming growth factor β
Thr	threonine
TKI	tyrosine kinase inhibitors
Tyr	tyrosine
UO126	1,4-diamino-2,3-dicyano-1,4-bis[2-aminophenylthio]butadiene
UV	ultraviolet
WST-1	water soluble tetrazolium salt 1
XP	Xeroderma pigmentosum

1 Introduction

1.1 Cutaneous squamous cell carcinoma (cSCC)

Traditionally, skin cancers are grouped into two categories: melanoma and non-melanoma skin cancers (NMSC). Cutaneous squamous cell carcinoma (cSCC) is the second most common non-melanoma skin cancer after basal cell carcinoma (BCC). cSCC represents 20 % of all NMSC and its incidence is increasing worldwide (Lomas et al. 2012). It accounts for 20 % of deaths from skin cancer (Gurney and Newlands 2014).

cSCC is a tumor of the elderly population with 80 % of cases reported in individuals older than 70 years (Garcovich et al. 2017). This can explain the increasing incidence of cSCC with increasing life expectancy.

The main risk factor of cSCC is cumulative ultraviolet (UV) exposure. Australia is reported to have the highest average incidence of cSCC with 387 new cases per 100,000 person/years (Staples et al. 2006). This can be explained by the exposure to high UV-radiation in Australia due to the depletion of the ozone layer (Chipperfield et al. 2015). Pale skin (Fitzpatrick skin types I and II) also increases the risk of cSCC, whereas cSCC is uncommon in dark-skinned individuals. Greater amounts of melanin in the epidermis of the dark skin presumably protect against UV-light. Albinism, which is a genetic defect of melanin production, is associated with an increased risk of cSCC (Diepgen and Mahler 2002). Another genetic disorder linked with cSCC is Xeroderma pigmentosum (XP). It is a rare autosomal recessive disorder in which nucleotide excision repair enzymes are mutated. This leads to a decreased ability to repair DNA damage caused by UV-light. Patients with XP usually develop skin cancers at a very young age (Lichon and Khachemoune 2007). The link between UV light and cSCC is also demonstrated by a study showing an increased risk of cSCC development in psoriasis patients who were treated with psoralen and UV-A (PUVA) therapy (Stern 2012).

The effect of UV radiation on cSCC development can be explained by UV-induced immunosuppression. There are several possible mechanisms discussed in the literature on how UV radiation can influence the immune system. One of the explanations is that UV-light reduces the amount of effector T-cells, shifting the balance between regulatory and effector T-cells in favor of regulatory T-cells, which leads to suppression of the immune response (Elmets et al. 2014). In mice, it has been demonstrated that UV-induced skin tumors completely regress when transferred to a genetically identical immunocompetent recipient, but continue to grow when transferred to a genetically identical immunosuppressed host (Kripke 1974). It also has been observed that organ transplant recipients have a 65-250 times higher risk of cSCC development than the general population (Euvrard et al. 2003), which is possibly due to the following long-term immunosuppression. Not only immunosuppressed patients but also lymphoma and chronic lymphocytic leukemia patients have defects in cellular immunity and are predisposed to develop skin cancers including cSCC (Maule et al. 2007).

Genus-β of Human papillomavirus (β-HPV) is also thought to be linked with cSCC. However, although 30 % of cSCC are positive for β-HPV DNA, ultra-high-throughput transcriptome sequencing did not identify the expression of papillomavirus mRNA in any of them (Arron et al. 2011). Considering that the β-HPV DNA load is higher in precancerous actinic keratosis (AK) than in cSCC itself, it is suggested that β-HPV plays a role in tumor induction but is dispensable for tumor maintenance (Weissenborn et al. 2005).

cSCC originates from epidermal keratinocytes. AK is regarded as a precancerous skin lesion that progresses into cSCC. Usually, patients have AK at multiple sites and have a lifetime risk of developing cSCC between 6 % and 10 % (Salasche 2000). It may be inefficient to treat every single AK lesion, but patients with multiple AK lesions are advised to get follow-up examinations and, eventually, therapy in order to prevent progression to cSCC (Alam and Ratner 2001). Therapy options for AK include cryotherapy, electrodesiccation and curettage, 5-fluorouracil and imiquimod (Uhlenhake 2013). Other premalignant lesions that may progress to cSCC are actinic cheilitis (AC), which usually develops on the lower lip as a white papule or plaque, or keratoacanthoma, which arises from surgical scars or trauma (Kallini et al. 2015).

The main treatment option for cSCC is surgical excision. In 95 % of cases, the primary tumor is completely removed when excised with a minimum margin of 4 mm, but for tumors that are >2 cm, surgical excision with a minimum margin of 6 mm is recommended (Brodland and Zitelli 1992). More effective than standard surgical excision but more time-consuming and expensive is Mohs micrographic surgery (MMS). It is especially effective in recurrent cSCC lesions. When treated with standard excision, 23.3 % of recurrent cSCC recur, whereas MMS results in a recurrence rate of only 10 % (Rowe et al. 1992). Other therapeutic modalities used in cSCC treatment are electrodesiccation and curettage, radiotherapy, and photodynamic therapy.

Despite surgical therapy being generally successful, a 10-years retrospective study shows a 3.7 % risk of metastasis and a 2.1 % risk of disease-specific death (Schmults et al. 2013). The most common site of metastasis is the parotid gland and, in such cases, superficial parotidectomy with following adjuvant radiation is recommended (Miller 2000).

Several molecular changes have been associated with cSCC. These include mutations in *p53*. *p53* encodes for a protein that functions as a tumor suppressor by regulating the cell cycle. One study shows that 69 % of cSCC samples are positive for *p53* mutations. Most of the mutations were C to T transition mutations, which are characteristic of UV-induced DNA damage. As *p53* mutation rate is higher in cSCC than in precancerous AK, it is thought that *p53* is involved in the conversion of AK to cSCC (Nelson et al. 1994). Other signaling pathways engaged in cSCC are the Wnt/β-catenin- and the calcium- and integrin signaling pathways (Ra et al. 2011). Wnt-proteins are ligands that bind to frizzled (FZD) receptors. This leads to the stabilization of β-catenin, which is transported to the nucleus where it forms complexes with TCF/LEF and activates expression of Wnt target genes, including the well-known oncogene c-Myc (Logan and Nusse 2004). Calcium is a ubiquitous second messenger that is important for many cellular processes. Calcium signaling is implicated in carcinogenesis by evading apoptosis (Capiod et al. 2007). Calcium is also involved in epidermal differentiation (Bikle et al. 2004). Integrins are transmembrane cell adhesion receptors that are known to mediate cell proliferation and apoptosis in cancer cells via different signal transduction pathways. Overexpression of some integrins is associated with poor prognosis in cervical squamous cell carcinoma and colon carcinoma (Bates et al. 2005; Hazelbag et al. 2007). In cSCC, aberrant expression of integrins is implicated in the

proliferation of stem cells in the underlying basal layer of cancer tissue (Janes and Watt 2006).

Besides, the HH and EGFR signaling pathways are involved in cSCC pathology, which is discussed in detail below (see section 1.4.2).

1.2 The Hedgehog (Hh) signaling pathway

The Hedgehog (Hh) signaling pathway was at first described by Christiane Nüsslein-Volhard and Eric Wieschaus, who were awarded with the Nobel Prize for their work in 1995. Nüsslein-Volhard and Wieschaus discovered mutations that are affecting the segment number and the anterior-posterior body axis in Drosophila. They identified 15 different genes, which when mutated caused disturbances in the formation of the body axis or in the segmentation pattern. These genes were grouped into three classes. The first class includes gap genes that affect the number of body segments. Pair rule genes influence every second body segment and mutations in these genes lead to an embryo consisting of only odd-numbered segments. The third class consists of segment polarity genes, which are important for head-to-tail polarity (Nüsslein-Volhard and Wieschaus 1980). The mutation of one of these genes led to a hedgehog-like appearance of Drosophila what inspired the name of the gene *Hedgehog* (*Hh*). Later, gene homologs were found in other species and it was discovered that principles described in Drosophila also apply to higher animals and humans. This led to the conclusion that the basic mechanism of embryological development is evolutionary conserved.

The important role of the Hedgehog signaling pathway in embryological development is obvious. However, today it is known that this pathway is active also in adult cells to maintain organ homeostasis and to repair injured tissue (Petrova and Joyner 2014).

The expression of the transcription factor *GLI1* is the main read-out of HH signaling pathway activity and *GLI1* level can be affected by both canonical and non-canonical HH signaling.

1.2.1 Canonical Hh signaling

The main components of canonical Hh signaling are the Hh ligands, the Hh receptor Patched1 (Ptch) and its signal transduction partner Smoothened (Smo) and the transcription factors of the glioma-associated oncogene (Gli) family. Hh ligands are secreted glycoproteins. In mammalians, there are three groups of Hh ligands: Sonic hedgehog (Shh), Indian hedgehog (Ihh) and Desert hedgehog (Dhh). Shh is the most studied HH ligand. It plays an important role in the development of the neural tube and is expressed in the node, notochord and the floor plate (Briscoe et al. 2001). The deletion of *Shh* leads to cyclopia (Chiang et al. 1996). Ihh is expressed in chondrocytes (St-Jacques et al. 1999) and homozygous mutations lead to acrocapitofemoral dysplasia, which is an autosomal recessive disorder characterized by bone defects (Hellemans et al. 2003). Dhh is particularly expressed in the gonads and male mice homozygous for Dhh mutation are infertile (Bitgood et al. 1996).

The precursor molecule of the Hh ligand has a signal peptide at the N-terminal domain, which directs the protein into the lumen of the endoplasmic reticulum. Here the signal peptide is removed and a palmitoylation reaction is catalyzed by Hh acetyltransferase (Hhat) (Pepinsky et al. 1998; Buglino and Resh 2008). In addition, the C-terminal domain of the precursor catalyzes a reaction that provides the N-terminal domain of the Hh ligand with a cholesterol moiety (Porter et al. 1996). After this modification, the C-terminal domain is cleaved by ER-associated degradation (ERAD) (Chen et al. 2011). Unimpaired processing of Hh is essential for the normal function of Hh signaling. This is seen especially in patients with holoprosencephaly that can be caused by mutations in human SHH leading to aberrant SHH processing (Traiffort et al. 2004). The cholesterylated Hh ligand is highly lipophilic and needs a special transmembrane protein named Dispatched (Disp) that mobilizes the ligand from plasma membrane (Burke et al. 1999). To be transported to the target cell the Hh ligand needs to bind to extracellular chaperones. In vertebrates, these chaperons belong to the Scube family (Johnson et al. 2012). On the surface of the receiving cell, the Hh ligand binds to its receptor Ptch and inhibits it. There are data suggesting that other coreceptors are also essential for Hh binding to Ptch (Yao et al. 2006). Ptch is a 12-pass transmembrane protein. In the absence of the Hh ligand, Ptch inhibits its interaction partner Smo, which is another transmembrane protein. Binding of the Hh ligand to Ptch suspends the inhibition of Smo

and leads to activation of this protein. It is not yet clear by which molecular mechanism Ptch inhibits Smo, but it has been suggested that Ptch promotes dephosphorylation and thus inactivation of Smo (Jia et al. 2004). The 7-pass transmembrane protein Smo furthermore has a small-molecule-binding site that can be occupied by antagonists like the synthetic Smo antagonist (SANT1), cyclopamine and vismodegib or by agonists like the smoothened agonist (SAG) (Chen et al. 2002). Downstream of Smo there is a complex of proteins, including protein kinase Fused (Fu), Suppressor of Fused (SuFu) and kinesin-related protein costal2 (Cos2). Cos2 serves as a scaffold (Lum et al. 2003). Fu activates Hh signaling, while SuFu acts as an inhibitor. This protein complex regulates the expression of a transcription factor Cubitus interruptus (Ci) in drosophila. In vertebrates Gli1, Gli2 and Gli3 are the homologs of Ci. In the absence of the Hh ligand, Ci exists as a protein with the low intrinsic transcriptional activity that has been proteolytically processed from the full-length form and lacks C-terminal activator domain. When Hh signaling is activated, the full-length form of Ci accumulates and gets modified into its active form, which promotes the transcription of the target genes (Ohlmeyer und Kalderon 1998).

Target genes of the HH signaling pathway include Ptch itself and the hedgehog interacting protein (Hhip). Hhip attenuates Hh signaling by binding to Hh proteins (Chuang und McMahon 1999). Expression of Ptch and Hhip as a result of Hh signaling activation is an example of a negative feedback loop regulation of signaling pathways.

A very simplified schematic representation of the canonical HH signaling pathway in its ON- and OFF-states is shown in Figure 1.

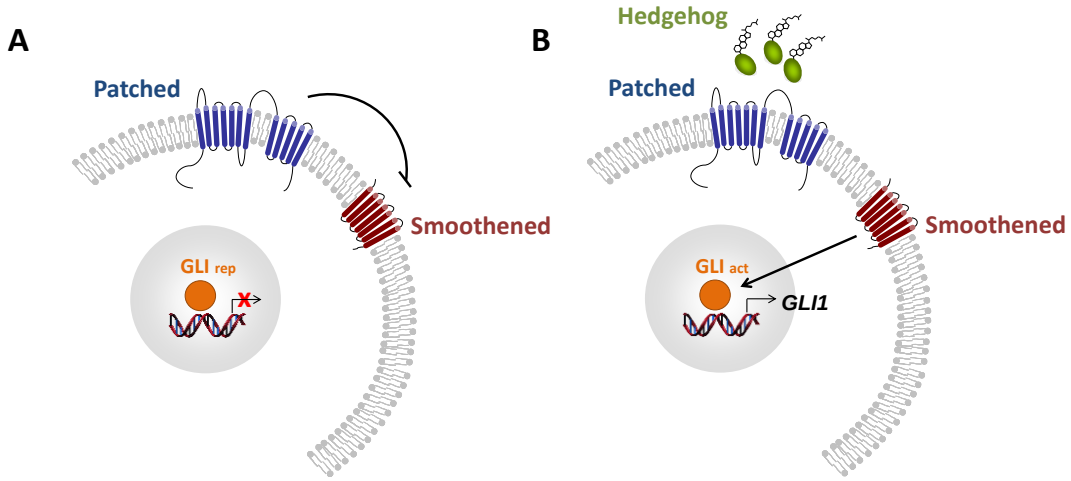

Figure 1: Schematic representation of the canonical Hedgehog signaling pathway. Major components of the pathway are the Hedgehog ligand, the 12-pass transmembrane receptor Patched, the 7-pass transmembrane signal transduction protein Smoothened and GLI transcription factors as a repressor (GLI_{rep}) and activator (GLI_{act}) forms. GLI1 transcription is the main readout of the pathway's activity. **A.** Without the Hedgehog ligand Patched inhibits Smoothened and the GLI_{rep} is generated. It is translocated into the nucleus and inhibits the transcription of target genes. **B.** When Hedgehog binds to Patched, the inhibition of Smoothened is abolished, GLI_{act} forms are stabilized and translocated into the nucleus, where they stimulate transcription of target genes (modified from Pyczek 2018).

1.2.2 Canonical HH signaling in cancer

The components of the canonical HH signaling are involved in different entities of cancer. There are two mechanisms of how active HH signaling can lead to cancer, which involve either a ligand-dependent or a ligand-independent activation of the pathway.

Ligand-dependent activation of the HH signaling pathway can be based on autocrine signaling. In this scenario, the tumor cells secrete abnormal amounts of the HH ligand, which stimulates the pathway in the tumor cells themselves. The ligand-dependent activation can also be paracrine, which means that HH ligands produced by tumor cells affect stromal cells of the tumor microenvironment (reviewed in (Scales und de Sauvage 2009)). Autocrine stimulation of HH signaling in tumors has been reported in lung, colorectal, esophageal, pancreas cancers and in melanoma (Yuan et al. 2007; Qualtrough et al. 2004; Ma et al. 2006; Thayer et al. 2003; Stecca et al. 2007). Paracrine stimulation of HH signaling was first described in prostate cancer (Fan et al. 2004) and later for pancreatic and colorectal cancer

(Yauch et al. 2008). A third mechanism of ligand-dependent activation of the HH signaling pathway is the so-called "reversed paracrine" model, where HH ligands are secreted from stromal cells to receiving tumor cells. This model has been observed in B- and plasma cell malignancies (Dierks et al. 2007).

Ligand-independent activation of the HH signaling pathway is based on mutations. This mechanism was first shown in nevoid basal cell carcinoma syndrome (NBCCS), also known as Gorlin syndrome. Gorlin syndrome is an autosomal dominant disease characterized by developmental abnormalities and a predisposition to neoplasms, including multiple basal cell carcinomas (BCC) and medulloblastoma (MB). Patients with Gorlin syndrome have heterozygous *PTCH* germline mutations (Hahn et al. 1996). Mutations in *PTCH* gene are also found in sporadic BCC. Because these tumors very frequently show loss of both *PTCH* alleles, *PTCH* is considered to be a tumor suppressor gene. Moreover, as seen in several mouse models dysregulation of Hh signaling is essential for BCC proliferation and survival e.g. see (Hutchin et al. 2005). *PTCH1* or *SuFu* mutations are frequently found in MB (Raffel et al. 1997; Taylor et al. 2002) and have also been reported in rhabdomyosarcoma (RMS) (Tostar et al. 2006).

Mutations of HH signaling pathway members have also been described in cSCC. 15 % of cSCC show *PTCH* mutations (Ping et al. 2001). In another study allelic loss of *PTCH* was detected in 50 % of cSCC tumors (Danaee et al. 2006). Immunohistochemical analysis of SCC samples showed positive nuclear staining of GLI1 in 12,5 % of cases (Tanese et al. 2018). All these data indicate a potential involvement of the HH signaling pathway in cSCC.

Because of the overactivation of canonical HH signaling in a lot of different malignancies, inhibition of the HH pathway has been of high interest for medical scientists. The first HH pathway inhibitor that was used in the research was cyclopamine. Cyclopamine is a naturally occurring steroidal alkaloid that can be isolated from corn lily *Veratrum californicum*. It shows teratogenic effects including cyclopia in lambs by binding to SMO and inhibiting the HH signaling pathway (Cooper et al. 1998; Chen et al. 2002). Because of cyclopamine's low affinity to SMO, low oral bioavailability and high toxicity, new inhibitors were synthesized. IPI-269609 that has higher bioavailability than cyclopamine, has shown promising results in pancreatic cancer (Feldmann et al. 2008). So far, there are only two HH pathway inhibitors that have been approved by the Food and Drug Administration (FDA). These are

vismodegib and sonidegib for locally advanced and metastatic BCC. Currently, there are several clinical trials in progress for using these drugs in other tumor entities. However, vismodegib and sonidegib are SMO-inhibitors and those tumors that result from mutations down-stream of SMO will not respond to these drugs.

1.2.3 Non-canonical Hh signaling

Non-canonical HH signaling can mean either GLI-independent functions of PTCH and SMO or regulation of GLI transcription factors without involvement of canonical components (reviewed in (Robbins et al. 2012)).

An example of non-canonical HH signaling is the GLI-independent induction of apoptosis by PTCH. Thus, it has been shown that the expression of Ptch in the absence of Shh leads to apoptosis induction (Thibert et al. 2003). Ptch also regulates the cell cycle in that it interacts with CyclinB1 suggesting a link between Gli1-independent tumor suppressor activity of Ptch and inhibition of cell division (Barnes et al. 2001). SMO also can act in a non-canonical way. SMO stimulates the small Rho GTPases Rac1 and RhoA thereby promoting fibroblast migration in a GLI-independent manner (Polizio et al. 2011). The involvement of SMO in Ca^{2+} signaling is also described in the literature (Belgacem and Borodinsky 2011).

PTCH- and SMO-independent regulation of GLI transcription factors includes GLI activation via the rat sarcoma protein (RAS) / rapidly accelerated fibrosarcoma protein (RAF) / mapk erk kinase (MEK) / extracellular signal-regulated kinase (ERK) and the phosphatidylinositol-3-kinase (PI3K) / protein kinase B (AKT) / mammalian target of rapamycin (mTOR) signaling pathways in different cancer entities.

1.2.4 Non-canonical HH signaling in cancer

There are lots of different reports suggesting non-canonical regulation of GLI transcription factors in various malignancies. One example is esophageal adenocarcinoma, in which

activated mTOR/S6K1 signaling enhances GLI1 transcriptional activity via S6K1-mediated GLI1 phosphorylation at Ser84 leading to release of GLI1 from its endogenous inhibitor SuFu (Wang et al. 2012). Subsequent experiments showed that DYRK1B kinase can mediate the interaction between the HH and mTOR pathways. Thus, it inhibits canonical HH signaling by blocking signal transduction from SMO to GLIs and promotes non-canonical HH signaling through activation of the mTOR/AKT pathway (Singh et al. 2017).

Other pathways that can regulate the activity of the GLI transcription factors are the WNT, NFκB, TGFβ, Notch, PI3K/AKT and EGF/EGFR signaling pathways.

The enhancement of GLI activity by the WNT/β-catenin pathway was observed in different human cancer cell lines of the stomach, colon, and lung. In these cancers transfection with β-catenin increased the transcriptional activity of GLI1 in a TCF/LEF-independent manner (Maeda et al. 2006). This has led to the suggestion to target both pathways simultaneously (Song et al. 2015). Similarly, a β-catenin-Gli1 interaction was also observed in medulloblastoma where it regulates proliferation and tumor growth (Zinke et al. 2015). Moreover, Insulin-like growth factor 2 mRNA-binding protein (IGF2BP1, also known as IMP1, CRD-BP, and ZBP1) that is a direct target of the canonical Wnt/β-catenin signaling pathway stabilizes GLI1 mRNA in BCC (Noubissi et al. 2009). Furthermore, knockdown of IGF2BP1 significantly reduced growth, proliferation, invasion capability and promoted apoptosis of a human BCC cell line (Noubissi et al. 2014).

The effect of the NFκB signaling pathway on the GLI transcription factors was shown in pancreatic ductal adenocarcinoma, in which the proinflammatory cytokines tumor necrosis factor-α (TNF-α) and interleukin-1β (IL-1β) lead to upregulation and nuclear localization of GLI1 and promote malignant cell behaviors including migration, invasion and epithelial-mesenchymal transition (EMT) (Wang et al. 2016).

PI3K/AKT signaling also can upregulate GLI1 and GLI2. This was observed in renal cell carcinoma and was negatively correlated with the patient's overall survival (Zhou et al. 2016). The PI3K/Akt/GLI1-axis is also active in osteosarcoma, where GLI1 seems to be indispensable for tumor cell survival (Zhu et al. 2018).

Notch signaling has also been reported to regulate GLI transcription factors. However, in contrast to other signaling pathways, this regulation is negative. One example is the depletion

of Notch1 in murine skin that results in increased expression of *Gli2*, causing the development of BCC-like tumors (Nicolas et al. 2003).

Because GLI transcription factors are effectors of HH signaling and apparently are very important for many different tumor features, several groups are attempting to develop agents to target GLI that would have wider applications than SMO inhibitors. Among GLI inhibitors are GANT58 and GANT61. Both show high selectivity for HH/GLI1 signaling and both act in the nucleus to block GLI function. GANT61 interferes with GLI1 DNA binding in living cells (Lauth et al. 2007). Arsenic trioxide (ATO) is another GLI inhibitor. ATO probably binds directly to GLI1 inhibiting its transcriptional function. It apparently also blocks the accumulation of GLI2 in cilia, ultimately resulting in reduced protein levels. ATO is an approved drug for the treatment of acute promyelocytic leukemia (Mastrangelo and Milani 2018). Therefore, it may provide an alternative treatment option for tumors with active HH signaling.

1.3 Epidermal growth factor/epidermal growth factor receptor (EGF/EGFR) signaling

The epidermal growth factor receptor (EGFR, HER1, ErbB1) belongs to the family of receptor tyrosine kinases (RTK). EGFR is the first discovered and the most studied RTK. EGFR is a transmembrane receptor that transduces signals to the cell interior and regulates many important functions including cell growth, proliferation, differentiation and homeostasis (reviewed in (Ceresa and Peterson 2014)).

Ligands of the EGFR include epidermal growth factor (EGF), transforming growth factor α (TGF-α), amphiregulin (AR) and epigen (EPG), which bind specifically to EGFR. Other ligands are epiregulin (EPR), betacellulin (BTC) and HB-EGF, which bind to both EGFR and ErbB4 (reviewed in (Hynes and MacDonald 2009)). EGF is the best-studied EGFR ligand. It was first isolated from the submandibular gland of mice in the 1960s and was reported to accelerate incisor eruption and opening of eyes of newborn mice by stimulating

the proliferation of epithelial cells (Cohen 1962). Subsequently, its human homolog, its receptor, and the receptor's intrinsic activity were identified (Carpenter et al. 1975; Ushiro and Cohen 1980). Cloning of EGFR led to a better understanding of the protein structure (Ullrich et al. 1984). Today it is known that EGFR has extracellular, transmembrane and intracellular segments. The extracellular segment has two ligand-binding and two cysteine-rich domains. The transmembrane segment consists of hydrophobic amino acids. The intracellular segment has a juxtamembrane domain, a tyrosine kinase domain and a C-terminus containing 20 tyrosine residues, of which seven are phosphorylated. When a ligand binds to EGFR, it homo- or heterodimerizes. This results in tyrosine kinase activity leading to auto-transphosphorylation of tyrosine residues at the C-terminus. The phosphorylated tyrosine residues serve as docking sites for downstream signaling molecules and activate different signaling pathways including RAS/RAF/MEK/ERK, PI3K/AKT and mTOR signaling (reviewed in (Ceresa and Peterson 2014; Wang 2017)).

1.3.1 RAS/RAF/MEK/ERK signaling

The RAS/RAF/MEK/ERK cascade is one of the downstream pathways activated by EGR/EGFR (reviewed in (Wee and Wang 2017)). After auto-transphosphorylation of EGFR, phosphorylated tyrosine residues bind to the growth factor receptor-binding protein 2 (GRB2) by its Src homology 2 (SH2) domain (Lowenstein et al. 1992). This leads to the activation of the son of sevenless (SOS) nucleotide exchange factor (Buday and Downward 1993). SOS activates RAS. RAS is a small guanosine triphosphatase that can exchange GDP to GTP (Boriack-Sjodin et al. 1998). RAS interacts with RAF via the latter's Ras-GTP-binding domain (RBD). RAF is activated by phosphorylation (Brtva et al. 1995) at Ser338 and Tyr341. In turn, MEK1/2 are activated by phosphorylation at Ser217 and Ser221 (Xiang et al. 2002; Bondzi et al. 2000). The only known physiological substrates of MEK1/2 are ERK1/2 (Roskoski 2012). MEKs activate ERKs by double-phosphorylation at Tyr204 and Thr202 residues. Unlike MEKs, ERKs have numerous substrates in the cytoplasm and the nucleus. In the cytoplasm, ERKs can activate the p90 ribosomal S6 kinase 1 (RSK1) (Richards et al. 2001), which can translocate into the nucleus and can

activate the proto-oncogene c-FOS (Anjum and Blenis 2008). In the nucleus, ERK can activate transcription factors including ELK-1, ETS, SP-1 and c-JUN, which can regulate important processes like cell cycle and proliferation (Wee and Wang 2017).

A simplified schematic representation of RAS/RAF/MEK/ERK activation by EGFR is presented in Figure 2.

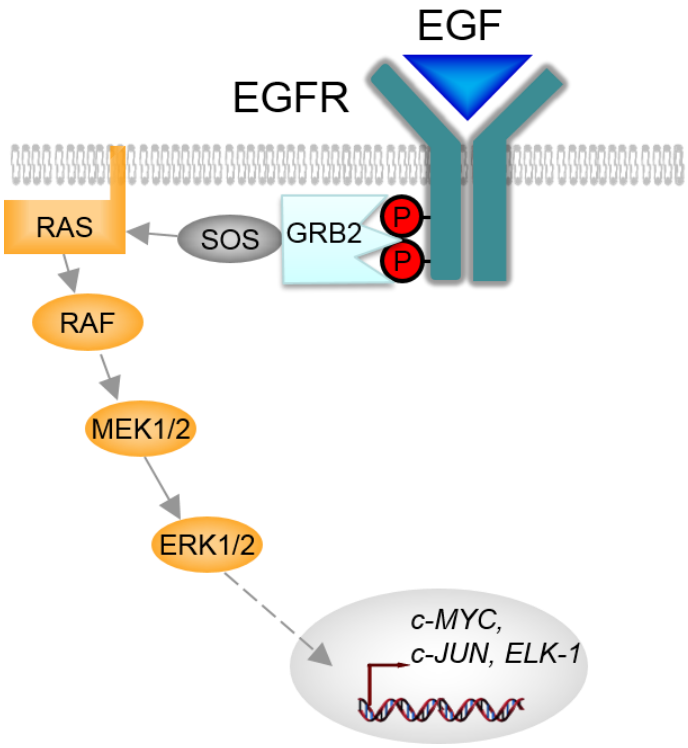

Figure 2: Simplified schematic representation of RAS/RAF/MEK/ERK activation by EGFR. Upon binding of the EGF ligand, EGFR dimerizes and autophosphorylates tyrosine residues. GRB2 docks at the phosphorylated tyrosine residues and recruits SOS that subsequently activates RAS. Activated RAS initiates the downstream signal cascade consisting of RAS/RAF/MEK/ERK, which leads to activation of transcription factors like c-MYC, c-JUN, and ELK-1 (modified from Wee und Wang 2017).

1.3.2 EGF/EGFR signaling in cancer

The EGF/EGFR signaling pathway plays a crucial role in many cancer entities. EGFR is frequently overexpressed or mutated in tumors (reviewed in (Lindsey and Langhans 2015)). Mutated *EGFR* can result in aberrant activity or in a constitutively active signaling pathway.

Constitutively active EGFR known as EGFRvIII that lacks the ligand-binding domain has been observed in 24 % to 67 % of glioblastoma and is considered to be a negative prognostic variable (Heimberger et al. 2005). EGFRvIII has also been reported in ovarian cancer (Moscatello et al. 1995), whereas other studies suggest that ovarian cancer samples are negative for EGFRvIII (Jungbluth et al. 2003; Steffensen et al. 2008). Similarly, contradictory data on EGFRvIII expression have been published for colon carcinoma (Cunningham et al. 2005; Azuma et al. 2006; Spindler et al. 2006). Mutations within the kinase domain of EGFR are present in up to 50 % of non-small cell lung cancer (NSCLC) samples that led to novel therapeutic options (Herbst et al. 2008). EGFR mutations are also seen in 15-30 % of breast cancer samples and are associated with poor clinical outcome (Hsu and Hung 2016). Moreover, constant EGFR activation is also detected in head and neck squamous cell carcinoma (HNSCC) (Weichselbaum et al. 1989).

Currently, there are two main options to therapeutically target constitutively active EGFR. The first group of drugs encompasses small-molecule tyrosine kinase inhibitors (TKI), which occupy the ATP-binding site of EGFR and thus inhibit its tyrosine kinase activity. Up to date, four TKIs have been approved by the FDA. The first approved TKI is Gefitinib. Gefitinib was approved in 2003 as a second-line treatment for NSCLC after cytotoxic therapies. In 2005 the FDA withdrew the approval due to lack of evidence that it extends life expectancy. However, Gefitinib was again approved by the FDA in 2015 as a first-line treatment for NSCLC. The second approved TKI was erlotinib as first-line treatment of NSCLC with exon-19 deletions or exon-21 L858R mutations. Erlotinib was also approved as a first-line treatment of pancreatic cancer in combination with gemcitabine. Lapatinib was approved as a second-line treatment for breast cancer. Afatinib was approved by FDA in 2014 as a first-line treatment of NSCLC with exon-19 deletions or exon-21 L858R mutations (Roskoski 2014). The second group of EGFR inhibitors are monoclonal antibodies, which bind to the extracellular ligand-binding site of EGFR and therefore inhibit the binding of the ligand. Cetuximab is one of them and has been approved for HNSCC and colorectal cancer without KRAS mutations. Panitumumab is another one and has been approved as a second-line treatment for metastatic colorectal cancer following cytotoxic therapies (Roskoski 2014).

1.4 Crosstalk between HH and EGF/EGFR signaling in cancer

A crosstalk between HH and EGF/EGFR signaling was suggested when a synergistic effect of both pathways in malignant transformation of human keratinocyte cells was observed. This synergistic effect apparently was mediated via activation of the MEK/ERK/JUN axis (Schnidar et al. 2009). Moreover, inhibition of both pathways synergistically reduced the growth of murine BCC cell lines with activated HH signaling (Schnidar et al. 2009). Furthermore, Shh-mediated proliferation of HeLa cancer cells and of neural stem cells involves EGFR internalization and ERK1/2 phosphorylation (Reinchisi et al. 2013). Finally, potential crosstalk between HH and EGF/EGFR signaling involving stabilization of GLI transcription factors through direct phosphorylation by ERK was suggested by computational prediction (Whisenant et al. 2010).

Together, these data show that the HH and EGF/EGFR signaling pathways can interact and potentiate each other's activity in different cancer entities.

1.4.1 HH and EGF/EGFR signaling pathways and potential crosstalk in cSCC

There are only a few data about the role of HH signaling in cSCC (please see section 1.2.2). However, our group recently found an inverse staining patter of GLI1 and pS6 in human cSCC samples by in-situ-hybridization and immunohistochemistry, respectively. Furthermore, the incubation of cSCC cell lines with EGF resulted in the downregulation of *GLI1*, which was reversed by co-treatment with the MEK inhibitor UO126. Moreover, incubation of cSCC cell lines with Hedgehog antagonist (HhA) went along with increased phosphorylation of ERK but with a downregulation of *GLI1* (Pyczek 2018). Altogether, these observations suggested a negative regulation of GLI1 by RAS/RAF/MEK/ERK signaling in cSCC.

After the approval of vismodegib for BCC treatment, several cases of BCC patients were reported who developed cSCC under treatment with vismodegib (Iarrobino et al. 2013; Orouji et al. 2014; Poulalhon et al. 2015; Saintes et al. 2015). As suggested by Saintes et al. it

is possible that tumor stem cells undergo squamous differentiation through inhibition of the HH pathway. To our knowledge, there are only two studies that investigated if BCC treatment with vismodegib increases the risk of cSCC. A case-control study including 180 patients showed an increased risk for cSCC after vismodegib therapy (Mohan et al. 2016). On the contrary, according to a retrospective cohort study including 1675 patients, vismodegib was not associated with an increased risk of cSCC when compared with standard surgical treatment of BCC (Bhutani et al. 2017).

There are only a few reports about the role of the EGF/EGFR signaling pathway in cSCC. In 2007 it has been reported that 43 % of cSCC samples express EGFR above background and that in most cases it is phosphorylated EGFR (Fogarty GB et al. 2007). Later in 2017, it has been published that EGFR overexpression in cSCC is associated with poor prognosis, including a higher rate of lymph node metastasis (Cañueto et al. 2017). In another study that supports this association, metastatic cSCC samples show stronger staining for EGFR than primary tumors (Shimizu et al. 2001). It has also been demonstrated that numerical aberrations of EGFR are very common in cSCC and are observed in 77 % of cases (Toll et al. 2010). Furthermore, it has been reported that TRAF6 forms a complex with CD147 and EGFR, inducing the malignant phenotype of cSCC by affecting cell growth and migration (Zhang et al. 2018). On the other hand, mutations in the *EGFR* gene are rare in cSCC and are only seen in 3 % of cases (Mauerer et al. 2011). Since EGFR is strongly expressed by cSCC, EGFR inhibition was assumed to be a promising therapeutic strategy in cSCC.

Until now, there has been a phase II study using cetuximab in patients with unresectable cSCC. In this study, cetuximab was successful, showing a 69 % disease control rate after six weeks (Maubec et al. 2011). However, only 36 patients have been enrolled in the study and therefore it is not possible to draw a definite conclusion about the benefit of cetuximab in cSCC patients. To our knowledge, there is no phase III study investigating the efficacy of cetuximab in cSCC.

1.5 Aim of the study

The general aim of the study was to investigate the role of HH signaling and its interaction with the EGFR-pathway in cutaneous squamous cell carcinoma. For this purpose, the cSCC cell lines MET-1, MET-4 and SCL-1 were used.

The first aim of this thesis was to analyze whether the EGF/MEK-associated inhibition of GLI1 expression was mediated by ERK. For this purpose, the cSCC cell lines were incubated with EGF and the ERK1/2-specific inhibitor SCH772984. We also assessed the impact of ERK inhibition on proliferation and metabolic activity of the cells.

Another aim was to investigate the role of (EGF-mediated) GLI1-downregulation in migration. For this purpose, the cells were treated with EGF or with *GLI1*-specific siRNA. To assess the migratory capacity of the cells, the insert migration assay was used.

We also tried to investigate the impact of GLI1 on epithelial-to-mesenchymal transition (EMT) by analyzing the expression of the mesenchymal markers *ZEB1*, *ZEB2*, *TWIST*, *VIM*, *SNAIL* and the epithelial marker *E-cadherin* (*CDH*). The expression of EMT-markers was measured in *GLI1*-knockdown, EGF-treated, and GLI1-overexpressing cells.

2 Material and methods

2.1 Material

2.1.1 Technical equipment

Table 1: List of laboratory equipment

Equipment	Supplier
- 20 °C Freezer	Liebherr GmbH, Ochshausen
- 80 °C Freezer (MDF-U71V)	Sanyo Electric Co., Ltd., Japan
4 °C Fridge	Robert Bosch GmbH, Stuttgart
Autoclave (Systec DX-150)	Systec GmbH & Co. KG, Linden
Biophotometer (6131)	Eppendorf AG, Hamburg
Centrifuges (Biofuge pico, fresco, primo, multifuge 3LR)	Kendro Laboratory Products GmbH, Hanau
Digital photo camera (PowerShot G2)	Canon Deutschland GmbH, Krefeld
Electronic pipettor (Accu-jet)	Brand GmbH & Co. KG, Wertheim
Electrophoresis System (XCell4 SureLockTM Midi-Cell)	Invitrogen GmbH, Karlsruhe
Freezing Container (Mr. FrostyTM)	Thermo Fisher Scientific GmbH, Schwerte
Heating block (Thermomixer)	Eppendorf AG, Hamburg
Heating stirrer (MR 3000/3001)	Heidolph Instruments GmbH & Co. KG, Schwabach
High-precision scales (Sartorius Basic plus)	Sartorius AG, Göttingen
Hybridization oven (HB-1000 Hybridizer)	UVP, Inc., Upland, USA
Imaging system Fluorchem Q	Fisher Scientific GmbH, Schwerte
Incubator (6000, BBD 6220)	Kendro Laboratory Products GmbH, Hanau

Inverted tissue culture fluorescence microscope (Axiovert 25)	Carl Zeiss Jena GmbH, Jena
Liquid nitrogen tank	L'air liquid S.A., Paris, France
Microplate reader (Synergy Mx)	BioTek Instruments, Inc., Bad Friedrichshall
Microscope (Olympus BX 60)	Olympus Deutschland GmbH, Hamburg
Mini centrifuge	Carl Roth GmbH & Co. KG, Karlsruhe
Orbital shaker (Unimax 1010)	Heidolph Instruments GmbH & Co. KG, Schwabach
pH-meter (inoLab pH Level 1)	WTW GmbH, Vienna, Austria
Pipettes (Multipette, One-channel)	Eppendorf AG, Hamburg
Power supply for electrophoresis	Peqlab Biotechnology GmbH, Erlangen
Real-Time PCR System (ABI Prism 7900HT)	Life Technologies GmbH, Darmstadt
Scale (Sartorius Basic plus)	Sartorius AG, Göttingen
Spectrophotometer (NanoDrop 8000)	Thermo Scientific, Wilmington, USA
Sterile bench (Euroflow Class IIA)	Clean Air Techniek bv, Woerden, Netherlands
Trans-Blot SD semi-dry transfer cell	Bio-Rad Laboratories GmbH, Munich
Vortexer-Genie 2	Scientific Industries, Woburn, USA
Water purification system (Arium® 611 VF)	Sartorius AG, Göttingen

2.1.2 Consumables

Table 2: List of consumable material

Consumer good	Supplier
1.5 ml reaction tubes	Ochs GmbH, Bovenden/Lenglern
1.5 ml safeseal microtubes	Sarstedt AG & Co., Nürnberg

2.0 ml reaction tubes	Sarstedt AG & Co., Nürnberg
15 ml falcon tubes	Greiner Bio-One GmbH, Frickenhausen
50 ml falcon tubes	Greiner Bio-One GmbH, Frickenhausen
6-well tissue culture plate	Sarstedt AG & Co., Nürnberg
24-well tissue culture plate (notched)	Corning Inc., Corning, USA
96-well assay plate (black)	Life Technologies GmbH, Darmstadt
96-well assay plate (transparent)	Corning Inc., Corning, USA
Blotting paper (GB 33 B003)	Heinemann Labortechnik GmbH, Duderstadt
Cell culture dishes (100 mm)	Nunc GmbH & Co.KG, Wiesbaden
Cell culture inserts (24-well, 8 µm)	BD Biosciences GmbH, Heidelberg
Cell scraper	Sarstedt AG & Co., Nürnberg
Combitips (0.2, 0.5, 2.5, 5, 10, 25, 50 ml)	Eppendorf AG, Hamburg
CryoPure tubes	Sarstedt AG & Co., Nürnberg
Cuvette (UVette)	Carl Roth GmbH & Co. KG, Karlsruhe
Filter tips (10 µl)	Sarstedt AG & Co., Nürnberg
Filter tips (100 µl, 200 µl, 1000 µl)	Kisker Biotech GmbH & Co. KG, Steinfurt
Neubauer counting chamber	Brand GmbH & Co KG, Wertheim
Nitrocellulose membrane (Hybond ECL)	GE Healthcare Europe GmbH, Freiburg
NuPAGE Novex 4-12 % Bis-Tris Midi Gel	Invitrogen GmbH, Karlsruhe
Pipette tips (10 µl, 200 µl)	Ochs GmbH, Bovenden/Lenglern
Pipette tips (20 µl, 1000 µl)	Sarstedt AG & Co., Nürnberg
QPCR adhesive clear seal	4titude Ltd., Berlin
Scalpel blade (#10, #24)	Aesculap AG & Co.KG, Tuttlingen
Serological pipettes (2 ml, 5 ml, 10 ml, 25 ml)	Sarstedt AG & Co., Nürnberg
Sterile filter	Omnilab-Krannich, Göttingen

2.1.3 Reagents and chemicals

Reagents and chemicals that are not listed below were purchased from Sigma-Aldrich Chemistry GmbH, Steinheim; AppliChem GmbH, Darmstadt, or Carl Roth GmbH & Co. KG, Karlsruhe.

Table 3: List of reagents and chemicals

Chemicals and reagents	Supplier
Ampuwa	Fresenius Kabi Deutschland GmbH, Bad Homburg
Bovine serum albumin (BSA)	Carl Roth GmbH & Co. KG, Karlsruhe
Deoxyribonucleotide triphosphate (dNTP)	Roche Diagnostics GmbH, Mannheim
Dithiothreitol, 100 mM (DTT)	Invitrogen GmbH, Karlsruhe
DNase/RNase-free distilled water	GIBCO Invitrogen GmbH, Karlsruhe
Ethanol (EtOH) 99 %	J.T. Baker B.V., Deventer, Netherlands
Ethanol (EtOH) 99 % denatured	CVH Chemie-Vertrieb GmbH & Co., Hannover
Ethylenediaminetetraacetic acid (EDTA)	ICN Biochemicals Inc., AuRORa, USA
Methanol	Carl Roth GmbH & Co. KG, Karlsruhe
Milk powder	Carl Roth GmbH & Co. KG, Karlsruhe
NuPAGE MES SDS Running Buffer, 20 x	Invitrogen GmbH, Karlsruhe
PBS-Tablets	GIBCO Invitrogen GmbH, Karlsruhe
Phosphatase inhibitor cocktail tablets (PhosSTOP)	Roche Diagnostics GmbH, Mannheim
Protease inhibitor cocktail tablets	Roche Diagnostics GmbH, Mannheim
Random Hexamer-Oligonucleotides	Invitrogen GmbH, Karlsruhe
SeeBlue® Plus2 Pre-Stained Standard	Invitrogen GmbH, Karlsruhe

Sodiumdodecylsulfate (SDS)	Carl Roth GmbH & Co. KG, Karlsruhe
tris(hydroxymethyl)aminomethane (Tris)	AppliChem GmbH, Darmstadt
TRIzol Reagent	Invitrogen GmbH, Karlsruhe
Tween-20	Scharlau Chemie S.A., Barcelona, Spain
Water-soluble tetrazolium salt-1 (WST-1) reagent	Roche Diagnostics GmbH, Mannheim

2.1.4 Kits and ready-to-use reaction systems

Unless stated otherwise, all the kits and ready-to-use reaction systems were used according to the supplier's instructions.

Table 4: List of kits and ready-to-use reaction systems

Reaction system	**Supplier**
Amersham ECL PlusTM Western Blotting Detection Reagents	GE Healthcare Europe GmbH, Freiburg
Cell Proliferation ELISA, BrdU (chemiluminescent)	Roche Diagnostics GmbH, Mannheim
HiPerFect transfection reagent	Qiagen GmbH, Hilden
Pierce BCA Protein Assay Kit	Thermo Fisher Scientific GmbH, Schwerte
Pierce ECL Western Blot substrate	Thermo Fisher Scientific GmbH, Schwerte
Platinum SYBR Green qPCR SuperMix	Invitrogen GmbH, Karlsruhe
Reverse Transcriptase (SuperScriptII®)	Invitrogen GmbH, Karlsruhe
RotiFect transfection reagent	Carl Roth GmbH & Co. KG, Karlsruhe

2.1.5 Buffers and solutions

Unless stated otherwise, all the buffers and solutions were prepared using double-distilled water (ddH_2O).

Table 5: List of buffers and solutions

Buffer or solution	Composition
Blotting buffer	20 % (v/v) Methanol 6 % (w/v) Tris 3 % (w/v) Glycine 0.0375 % (v/v) SDS
BSA/sodium azide solution	0.02 % sodium azide 2 % BSA in PBST
Modified RIPA buffer	50 nM Tris/HCl pH 7.4 1 % NP-40 0.25 % Na-Deoxycholat 150 mM NaCl 1 mM EDTA 1 protease inhibitor cocktail tabler per 10 ml 1 PhosSTOP tablet per 10 ml
PBS (cell culture)	1 PBS tablet in 500 ml ddH_2O
PBS-Tween-20 (PBST)	0.1 % Tween-20 in PBS
Phosphate buffered saline solution, 10 x, pH 7.4 (PBS, stock solution)	1.4 M NaCl 27 mM KCl 15 mM KH_2PO_4 65 mM Na_2HPO_4
Stripping buffer	62.5 mM Tris pH 6.7 2 % SDS 100 mM ß-Mercaptoethanol

2.1.6 Media

Table 6: List of cell culture media and reagents

Medium or reagent	Supplier
Dulbecco´s Modified Eagle Medium (DMEM)	Gibco, Invitrogen GmbH, Karlsruhe
Fetal calf serum (FCS)	Gibco, Invitrogen GmbH, Karlsruhe
L-Glutamine	PAN Biotech GmbH, Aidenbach
Minimum Essential Medium Eagle	Gibco, Invitrogen GmbH, Karlsruhe
Non-essential Amino Acids (NEAA)	Gibco, Invitrogen GmbH, Karlsruhe
Penicillin (10.000 U/ml)/Streptomycin (10 mg/ml) (P/S)	PAN Biotech GmbH, Aidenbach
RPMI 1640 (RPMI)	Gibco, Invitrogen GmbH, Karlsruhe
TrypLE Express	Gibco, Invitrogen GmbH, Karlsruhe

2.1.7 Biological material

Table 7: List of cell lines with corresponding media and supplement

Cell line	Description	Medium	Supplement	Reference
MET-1	Human cSCC cell line, primary tumor	DMEM	10 % FCS, 1 % P/S	(Popp *et al.*, 2000)
MET-4	Human cSCC cell line, metastasis	DMEM	10 % FCS, 1 % P/S	(Popp *et al.*, 2000)
SCL-1	Human cSCC cell line	RPMI	10 % FCS, 1 % P/S, 2 mM L-Glutamine, 1 % NEAA	(Boukamp *et al.*, 1982)
DAOY	Human medulloblastoma cell line	MEM	10 % FCS, 1 % P/S	(Jacobsen *et al.*, 1985)

2.1.8 Synthetic DNA-oligonucleotides

All synthetic DNA-oligonucleotides (primers) for qRT-PCR were purchased from Eurofins MWG Operon, Ebersberg. 100 µM stock solutions were prepared with ddH_2O and stored at – 80 °C. The concentration of the working solution used for qRT-PCR was 10 µM.

Table 8: List of synthetic DNA-oligonucleotides and origin of cDNA used as positive control

Transcript	Primer sequence (5´-3´)	Location	Control cDNA
18S	Forward: CGCAAATTACCCACTCCCG Reverse: TTCCAATTACAGGGCCTCGAA	exon 1	Mouse embryo E12.5
hHPRT	Forward: GCTGGTGAAAAGGACCTCT Reverse: CACAGGACTAGAACACCTGC	exon 7 exon 9	RMS-13 (rhabdomyosarcoma cell line)
hGLI1	Forward: AGCTACATCAACTCCGGCCA Reverse: GCTGCGGCGTTCAAGAGA	exon 11 exon 12	RMS-13
hGLI2	Forward: AAGCCCTTCAAGGCGCAGTA Reverse: TCGTGCTCACACACATATGGCTT	exon 9 exon 10	RMS-13
hCDH1	Forward: GTGGAGTGGCTCCACAAATAC Reverse: ATCCTGCTGCCAGGTCAGTGT	exon 3 exon 4	MET-1
hSNAI1	Forward: TCGGAAGCCTAACTACAGCG Reverse: CCAGATGAGCATTGGCAGCG	exon 1 exon 2	RMS-13
hTWIST1	Forward: AGATTCAGACCCTCAAGCTGG Reverse: AGACCGAGAAGGCGTAGCTGA	exon 1 exon 1	BJ (human foreskin fibroblast cell line)
hVIM	Forward: AACCTGGCCGAGGACATCATG Reverse: GCGTTCAAGGTCAAGACGTG	exon 1 exon 3	RMS-13
hZEB1	Forward: GAGGATGACCTGCCAACAGAC Reverse: TGCATCTGACTCGCATTCATC	exon 2 exon 4	BJ
hZEB2	Forward: ACAAGCCAATCCCAGGAG Reverse: ACACTAGCTGGACTCGTCT	exon 1 exon 2	BJ

2.1.9 Synthetic RNA-oligonucleotides

siRNAs used for knock-down experiments are listed in Table 9.

Table 9: List of siRNA

siRNA	Target sequence	Supplier
GLI1 (ON-TARGETplus SMARTpool)	GCAAAUAGGGCUUCACAUA AGGCUCAGCUUGCUUGUGUGUAA GGACGAGGGACCUUGCAUU CAGCUAGAGUCCAGAGGUU	Dharmacon Inc., Lafayette, USA
Scrambled siRNA (AllStars negative)	proprietary	Qiagen GmbH, Hilden

2.1.10 Plasmids

Plasmids listed below were used for the transfection of the cell lines.

Table 10: List of plasmids

Plasmid name	Application	Reference or supplier
pcDNA4NLSMT-GLI1	overexpression of human *GLI1*	gift from Prof. Fritz Aberger
pcDNA4/TO	control plasmid for *GLI1* overexpression	gift from Prof. Fritz Aberger

2.1.11 Synthetic inhibitors and agonists

Table 11: List of inhibitors and agonists used in cell culture experiments

Inhibitor or agonist	Solvent	Concentration	Supplier
EGF	0.1 % BSA/10 mM acetic acid	100 ng/µl	R&D Systems, Inc., Minneapolis, MN, USA
GANT61	DMSO	30 µM	Sigma-Aldrich, Steinheim
SCH772984	DMSO	0.1 µM	Selleckchem, Munich

2.1.12 Antibodies

Table 12: List of primary antibodies used for Western Blot. Primary Antibodies were diluted in 2 % BSA / 0.02 % azide in PBS-T.

Target protein	Source	Dilution	Supplier
HSC70	Mouse, monoclonal	1:5000	Santa Cruz, sc-7298
MAP Kinase (ERK1 and ERK2)	Rabbit, monoclonal	1:1000	Sigma-Aldrich, M5670
pERK (Ser473)	Rabbit, monoclonal	1:1000	Cell Signaling, 193H12

Table 13: List of secondary antibodies used for Western Blot. Secondary antibodies were diluted in 5 % milk PBS-T.

Antibody	Source	Dilution	Supplier
Anti-Mouse/HRP	Sheep, polyclonal	1:5000	GE Healthcare, NA931
Anti-Rabbit/HRP	Goat, polyclonal	1:5000	Sigma-Aldrich, A0545

2.1.13 Software

Table 14: List of software used for data analysis

Software	Developer
AlphaView Q SA 3.2.2	Cell Bioscience, California, USA
SDS 2.2	Applied Biosystems, Darmstadt
GraphPad Prism 6	GraphPad Software, Inc., La Jolla, CA, USA
Microsoft Office 2010	Microsoft Co., Redmont, USA
Zotero	Center for History and New Media at George Mason University, USA

2.1.14 Databases

Table 15: List of used databases

Database	Homepage
BasicLocalAlignmentSearchTool (BLAST)	http://blast.ncbi.nlm.nih.gov/Blast.cg
Ensembl	http://www.ensembl.org/index.html
National Center for Biotechnology Information (NCBI)	http://www.ncbi.nlm.nih.gov/
Reverse complement	http://www.bioinformatics.org/sms/rev_comp.html

2.2 Methods

2.2.1 Molecular biology methods

2.2.1.1 RNA Isolation from cultured cells

For RNA isolation from cells cultured in 6-Well-plates, TRIzol reagent was used according to the manufacturers' instructions. If not stated otherwise, the samples were kept on ice to avoid degradation of RNA. After aspiration of the medium, cells were washed with 1 ml PBS per well. After the addition of 1 ml TRIzol, the suspension was transferred into a 2 ml reaction tube, which was vortexed for 2 min at the highest speed following incubation at room temperature for 5 min. Then, 200 µl chloroform were added and the tube was again vortexed for 15 sec. Following 3 min incubation at room temperature, cells were centrifuged for 10 min at 12 000 rpm at 4 °C. From the three visible phases, the upper one containing RNA was transferred into a new reaction tube. RNA was precipitated by adding 500 µl Isopropanol and stored at -20 °C overnight. On the following day, the tube was centrifuged for 30 min at 12 000 rpm at 4 °C. The supernatant was discarded and the pellet was washed twice with 70 % ice-cold ethanol by centrifugation for 15 min at 13 000 rpm at 4 °C. The pellet was dried for 5 min at room temperature and dissolved in 20 µl RNA-ase free water at 56 °C for 10 min at 500 rpm. In the end, the reaction tube was stored at -80 °C until use.

2.2.1.2 Photometric quantification of RNA

Isolated RNA was quantified using the spectrophotometer NanoDrop 8000. Optical density was measured at 260 nm (OD_{260}). Since an OD_{260} of 1.0 corresponds to 40 µg/ml of RNA, the concentration was calculated according to the following formula:

$$\text{Concentration } (\mu g/ml) = OD_{260} \times 40$$

As proteins have an absorption maximum at 280 nm, OD_{280} was also measured in order to determine the protein concentration in the sample. The ratio of OD_{260} and OD_{280} was then

used to determine the purity of the isolated RNA. An OD_{260}/OD_{280} ratio of ~2.0 was considered as pure.

2.2.1.3 Reverse transcription (cDNA synthesis)

Synthesis of complementary DNA (cDNA) was performed using the SuperScriptII reverse transcriptase Kit. Usually, 2 µg of RNA were diluted in 7 µl RNAase-free water and incubated with 5 µl random hexamer primers for 10 min at 70 °C. After that, 0.5 mM deoxynucleotides (dNTPs) and 10 mM dithiothreitol (DDT) were added in 7 µl 1st strand buffer. The sample was then incubated at room temperature for 10 min. Subsequently, 1 µl SuperScriptII reverse transcriptase corresponding to 100 U was added. The reaction tube was incubated at 42 °C for 1 h to activate SuperScriptII, and the enzyme was then inactivated by incubation at 70 °C for 10 min. The reaction tube was stored at -20 °C until use. Assuming that the efficiency of reverse transcription is approximately 50 %, the final concentration of cDNA was considered to be 50 ng/µl.

2.2.1.4 Quantitative Real-Time polymerase chain reaction (qRT-PCR)

For the quantification of cDNA, the fluorescently labeled DNA-intercalating dye SYBR Green from Qiagen was used. Each reaction had a volume of 10 µl, containing the following components:

Table 16: Components of qRT-PCR

Component	Volume
Water (RNA-ase free)	3.2 µl

Forward primer	0.4 µl in RNA-ase free water (0.4 µM end concentration)
Reverse primer	0.4 µl in RNA-ase free water (0.4 µM end concentration)
SYBR Green	4 µl
cDNA	2 µl (50 ng, for *18S* 0.35 pg)

The PCR program consisted of 40 cycles, each of them containing a denaturation, annealing and an elongation step. The thermal profile of the program is shown in Table 17.

Table 17: Thermal profile of qRT-PCR

Stage	Temperature (°C)	Duration (sec)
Denaturation	95	15
Annealing	60	30
Elongation	72	30

For calculating gene expression, the standard curve method was used. For this purpose, a 5-fold serial dilution was prepared from the samples containing a known concentration of control cDNA starting from 35 pg/µl for *18S* rRNA and from 10 ng/µl for all the other transcripts. The logarithm of the known cDNA concentration was plotted against the respective cycle threshold values. The derived trend line with the corresponding equation y=mx + b served to assess cDNA amount in each sample. Finally, the transcript levels of each sample were normalized to the expression of the housekeeper genes *18S* or *HPRT*. All samples were measured in biological triplicates, each of them measured in three technical

replicates. For data analysis, SDS 2.2.1, Microsoft Excel 2010 and GraphPad Prism 6 software were used.

2.2.1.5 Protein Isolation from cultured cells

Cells were washed once with PBS, harvested with a cell scraper and transferred into a 15 ml falcon tube. The remaining cells were washed from the plate with 1 ml PBS and the suspension was also added to the tube. The tube was then centrifuged for 5 min at 1 800 rpm at 4 °C. The supernatant was discarded, and the cell pellet was resuspended in 30 µl (for cells that have been grown in a well of a 6-well tissue culture plate) or in 100 µl PBS (for cells that have been grown in a cell culture dish of 100 mm). The suspension was then transferred into a 1.5 ml reaction tube and centrifuged for 5 min at 2 000 rpm at 4 °C. The supernatant was discarded, and the pellet was shock frozen in liquid nitrogen. Then 20 µl (for cells that have been grown in a well of a 6-well tissue culture plate) or 100 µl (for cells that have been grown in a cell culture dish of 100 mm) RIPA buffer were added and the cells were lysed on ice for 30 min. Afterwards, the lysates were centrifuged for 25 min at 12 000 rpm at 4 °C and the supernatant containing the proteins was transferred into a new reaction tube and stored at - 80 °C until use.

2.2.1.6 Photometric quantification of proteins (BCA assay)

Proteins were quantified using the bicinchoninic acid (BCA) assay. This method is based on the Biuret reaction, in which cupric ions (Cu^{2+}) are reduced to cuprous ions (Cu^{1+}) by amino acid residues of polypeptides. The reaction takes place in an alkaline medium. A single cuprous ion forms a chelate complex with two BCA molecules. The formed complexes show strong absorbance at a wavelength of 540 nm. Protein concentrations of the samples were measured by comparing the absorbance of the sample protein solution to the absorption of a solution with a known protein concentration. For this purpose, a standard curve of serially diluted bovine serum albumin (BSA) was built starting with a concentration of 2 000 µg/ml.

1 µl of the sample was pipetted in a 96-well plate in triplicates. 200 µl of freshly prepared substrate reagents containing BCA, NaOH, and copper (II) sulfate were added per well. In addition, no-template-controls (NTC) were included. The plate was then incubated for 30 min at 37 °C for complex formation. The reaction was measured in a photometer at the wavelength of 540 nm and protein concentration was calculated by Microsoft Excel 2010.

2.2.1.7 Western Blot

Identical amounts of proteins were diluted in water to a final volume of 20 µl and 4 µl of 6 x loading buffer was added. The samples were denatured in a shaker at 450 rpm and at 95 °C for 5 min. After a short spin-down, the samples were loaded on a NuPAGE 4-12 % Bis-Tris Midi Gel. SeeBlue Plus 2 Prestained Standard served as a marker. The proteins were separated at 160 mA and 160 V for 2 h in NuPAGE MES SDS running buffer.

After gel electrophoresis, proteins were blotted onto a nitrocellulose membrane using the semi-dry method. Prior to blotting, the membrane was dipped into distilled water, while Whatman papers were moistened in blotting buffer. The blotting of the proteins was done at 120 mA and 20 V for 1 h 20 min. The arrangement of the blotting components was as follow from above to below:

1. Cathode (-)
2. 2x Whatman paper
3. SDS-PAGE Gel
4. Nitrocellulose membrane
5. 2x Whatman paper
6. Anode (+)

After blotting, the membrane was blocked with 5 % milk PBS-T solution for 1 h at room temperature followed by 3 washing steps with PBS-T for 10 min at room temperature. Afterwards, the membrane was incubated with the primary antibody diluted in 2 % BSA / 0.02 % azide in PBS-T at 4 °C overnight. On the following day, the membrane was washed

with PBS-T three times for 10 min at room temperature and incubated with the secondary antibody (conjugated with horseradish peroxidase) dissolved in 5 % milk PBS-T for 1 h at room temperature. After washing three times the ECL Detection Reagents System was used for detection according to the manufacturer´s instructions. After 3 min of incubation with ECL Detection Reagents, the signals were detected with the FlourChemQ Imaging System. For the analysis of the images, AlphaView Q SA 3.2.2 was used.

If several proteins of a similar size were analyzed on the same membrane, the membrane was stripped. For this purpose, the membrane was incubated for 30 min at 50 °C in a stripping buffer. After washing 2 times for 10 min with PBS-T at room temperature, the membrane was again used for Western Blot analysis.

2.2.2 Cell biology methods

2.2.2.1 Culture of cells

All cell lines were cultured at 37 °C, 5 % CO_2, and 95 % humidity. The cells were washed with PBS and the media was refreshed at least every third day. When the confluency of the cells reached 80-90 %, the cells were seeded for the experiment or were split.

2.2.2.2 Passaging of cells

Cells were first washed with PBS and 1 ml (for a well of a 6-well tissue culture plate) or 3 ml (for a cell culture dish of 100mM) of TrypLe Express containing trypsin was added. Then the plate was incubated at 37 °C for 5 min till the cells got detached from the surface and trypsin was inactivated with 1 ml or 3 ml of culture medium containing serum. The suspension containing the detached cells was transferred into a falcon tube and the plate was washed with 1-4 ml of PBS to collect the rest of the cells. The falcon tube was centrifuged at 300 x g at 4 °C for 5 min. The supernatant was discarded. The cell pellet was resuspended

in fresh culture medium. After counting in a Neubauer chamber, the desired number of cells was seeded on a new cell culture plate.

2.2.2.3 Cryopreservation of cells

For long-term storage cells were cryopreserved in liquid nitrogen. For this purpose, the cells were cultured until they reached 80-90 % confluency. Then they were washed with PBS, detached with trypsin and collected by centrifugation (for detailed description see "Passaging of cells"). The collected cells were resuspended in 10 % DMSO-containing culture medium and stored in cryovials at -20 °C for one night and at -80 °C the following night. Finally, the cells were transferred into a liquid nitrogen tank.

For the thawing of the cells, the cryovial was placed in a warm water bath until the content became liquid. After that, the cell suspension was rapidly transferred into a falcon tube containing culture medium. After centrifugation at 300 x g at 4 °C for 5 min, the supernatant was discarded, and the pellet was resuspended in fresh culture medium. The suspension was transferred into the culture dish and the equal distribution of the cells was checked under the microscope. On the next day, the cells were washed with PBS and the culture medium was refreshed to ensure complete elimination of DMSO.

2.2.2.4 Incubation of cells with EGF

200 000 MET-1 or MET-4 or 150 000 SCL-1 cells/well were seeded in a 6-well-plate in complete medium. After 24 h complete medium was replaced with starvation medium containing only 0.5 % FCS. The aim of the starvation was to exclude the effects of growth factors included in the serum of the complete medium. After 24 h of starvation, the cells were treated with 100 ng/µl of EGF for 24 h and afterwards, RNA was isolated.

2.2.2.5 Transfection of cells with plasmid DNA

Plasmid DNA (pDNA) was transfected into cells using a Rotifect transfection reagent. For transfection, 200 000 cells/well were seeded onto a 6-well cell culture plate the day before. For each well of a 6-well culture plate a total of 2 µg pDNA was used. The stock concentration of pDNA was 1µg/µl. On the next day, pDNA and Rotifect were diluted separately in 200 µl base medium. The ratio of pDNA and Rotifect was 1:5 for MET-4 and 1:2 for SCL-1. pDNA and Rotifect were mixed by pipetting and then incubated for 40 min at room temperature to let pDNA and transfection reagent form complexes. In the meantime, the medium of the cells was replaced by 1.5 ml of antibiotic-free medium supplemented with 10 % FCS. Then the base medium containing pDNA and Rotifect was added dropwise onto the cells. After 3 - 12 h the medium was replaced with normal cell culture medium. Afterwards, RNA was isolated from the cells.

To estimate the efficiency of the transfection procedure, a plasmid expressing enhanced green fluorescent protein (EGFP) was transfected and the efficiency was assessed by fluorescence microscopy.

Unfortunately, we were not able to transfect MET-1 cells because the Rotifect method was too toxic for this cell line.

2.2.2.6 Transfection of cells with siRNA

Transfection with siRNA was done using the HiPerFect according to the manufacturer's instructions. For this purpose, 200 000 cells/well were seeded on a 6-well culture plate the day before transfection. The transfection mixture consisted of 300 ng siRNA, 18 µl of HiPerFect reagent and 400 µl of the base medium. This mixture was incubated for 10 min at room temperature. During that time siRNA formed complexes with HiPerFect transfection reagent. After having removed the medium and having washed the cells with PBS, the cells were incubated with fresh growth medium and the transfection mixture was added dropwise to the well and distributed evenly. The cells were then incubated for at least 24 h. After that time RNA was isolated from the cells.

2.2.2.7 Migration assay

The migratory capacity of the cells was estimated by a transwell cell migration assay. For this purpose, 100 000 cells/well were cultured in starvation medium (containing 0,5 % FCS and 1 % P/S) substituted with EGF or solvent on cell culture inserts with a pore size of 8 µm for 18 h in a 24-well cell culture plate containing starvation medium without EGF. After this time, inserts were placed in a new 24-well cell culture plate containing 5 µM calcein in 500 µl starvation medium/well for 1h. Afterwards, the inserts were washed with PBS three times to remove not migrated cells on top of the membrane. In the end, the number of migrated cells was estimated using fluorescent microscopy. For the image analysis, AlphaView Q SA 3.2.2 and GraphPad Prism 6 software were used.

2.2.2.8 Proliferation assay

The cell proliferation rate was measured by BrdU-incorporation-assay. BrdU (bromodeoxyuridine) is a synthetic thymidine analog that is incorporated in newly synthesized DNA during the S-phase of the cell cycle.

For BrdU-assay 6 000 cells were seeded into each well of a 96-well cell culture plate and grown for one day. On the next day, the cells were incubated for 24 h with BrdU and the desired concentration of an inhibitor in 10 % FCS, 1 % P/S medium. Then 200 µl per well FixDenat were added for 30 min at 15-25 °C. FixDenat was replaced with Anti-BrdU-POD, which is a BrdU-binding antibody coupled with peroxidase. After incubation for 60 min at room temperature, wells were washed with washing buffer three times for 5 min each. Meanwhile, the substrate solution for peroxidase was prepared by mixing components A and B of the kit at a ratio of 1:100. The substrate solution was aspirated by the machine and distributed at 100 µl among each well. BrdU incorporation and thus the proliferation rate was measured in a luminescence plate reader. Data analysis was performed using Microsoft Excel 2010 and GraphPad Prism 6 software.

2.2.2.9 Metabolic activity assay

The metabolic activity of the cells was assessed by the water-soluble tetrazolium salt (WST-1) assay. Only when cells have intact mitochondria, stable tetrazolium salt WST-1 is converted to soluble formazan, which can be measured at a wavelength of 450 nm. For WST-1 assay 6 000 cells were seeded per well of a 96-well culture plate and grown for one day. On the following day, the cells were incubated with the desired concentration of inhibitor at 37 °C. After 24 h of incubation 100 µl WST-1 staining solution were added per well for 3 h at 37 °C. After that absorption was measured at 450 nm and 655 nm. As the medium has an absorption maximum at 655 nm and formazan at 450 nm, the quotient of them was used to assess metabolic activity. All the samples were measured in triplicates. For data analysis, Microsoft Excel 2010 and GraphPad Prism 6 software were used.

3 Results

3.1 ERK and its role in EGF-mediated GLI1 downregulation in cSCC cells

As already stated in the introduction, EGF downregulates *GLI1* expression in cSCC cell lines via the MEK/ERK axis. This was shown by the treatment of the cells with the MEK inhibitor U0126. In order to figure out whether *GLI1* expression is regulated downstream of MEK by ERK1/ERK2, the experiments were performed with the ERK1/ERK2 inhibitor SCH772984 that inhibits phosphorylation of residues in the activation loop of ERK.

3.1.1 ERK inhibitor SCH772984 blocks phosphorylation of ERK

To check the functionality of SCH772984, the cells were incubated with different concentrations (0.1 – 10 µM) of the inhibitor for 24 h and the levels of ERK1/ERK2 and their phosphorylated forms (pERK) were measured via Western Blot. The results of the Western Blot are shown in Figure 1. Whereas the total ERK level did not change after treatment with SCH772984, phosphorylation was blocked even at the lowest used concentration (0.1 µM). The experiment was repeated three times and Figure 3 shows a representative experiment.

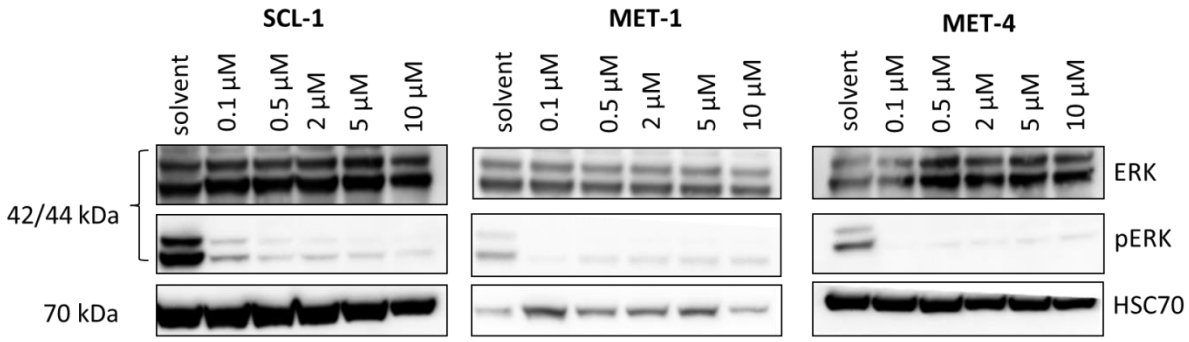

Figure 3: Impact of SCH772984 on ERK and pERK levels in SCL-1, MET-1 and MET-4 cell lines. Western Blot showing ERK and pERK levels in SCL-1, MET-1 and MET-4 cells that have been treated either with solvent or with 0.1 µM, 0.5 µM, 2 µM, 5 µM or 10 µM of SCH772984 for 24 h. HSC70 served as a loading control. Protein sizes in kDa are indicated on the left side of the blots.

To sum up, SCH772984 is able to inhibit the phosphorylation of ERK in all three cell lines already at a concentration of 0.1 µM. This concentration was used in all subsequent experiments.

3.1.2 SCH772984 upregulates *GLI1* expression

In order to examine the effect of ERK on *GLI1* expression, cSCC cells were incubated with SCH772984 for 24 h and *GLI1* expression was measured by qRT-PCR. As shown in Figure 4, SCH772984- treated cells express significantly more *GLI1* compared to solvent-treated control cells.

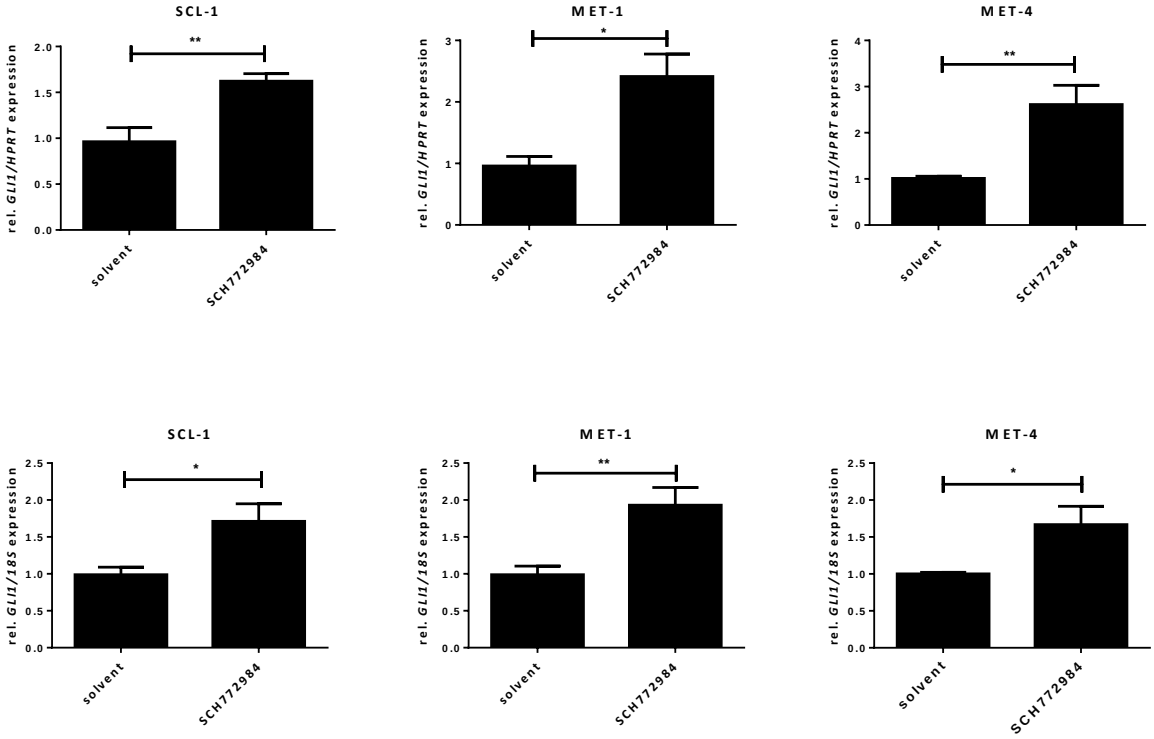

Figure 4: Effect of ERK inhibition on *GLI1* expression level in cSCC cell lines. qRT-PCR representing *GLI1* expression upon treatment with 0.1 µM SCH772984 for 24 h in SCL-1, MET-1 and MET-4 cells. The expression level was normalized to *HPRT* (upper panel) or *18S rRNA* (18S; lower panel). Gene expression data are shown as fold change to data of respective solvent- treated controls that were set to 1. Data are presented as mean values of three independent experiments measured in triplicates ± SEM; *, $p<0.05$; **, $p<0.01$. Statistical comparisons were done with Mann-Whitney test.

These results indicate that ERK inhibition leads to a significant upregulation of *GLI1* expression in cSCC cell lines.

3.1.3 SCH772984 upregulates *GLI1* expression in EGF-treated cSCC cells

To find out, if SCH772984 also upregulates *GLI1* expression in cSCC cells after EGF treatment, the cells were incubated concomitantly with EGF and the ERK-inhibitor SCH772984 for 24 h. As demonstrated in Figure 5 and as previously shown by our group, *GLI1* expression was significantly downregulated after incubation with EGF in all three cell

lines. The EGF-mediated downregulation of *GLI1* was reversed upon concomitant ERK-inhibition with SCH772984 in MET-1 and MET-4 cells and was restored to basal *GLI1* levels of the respective solvent treated cells (Fig. 5). A different pattern was observed in the cell line SCL-1. As seen in MET-1 and MET-4 cells, EGF downregulated *GLI1* expression. However, in contrast to MET-1 and MET-4, it remained significantly downregulated upon treatment with SCH772984 in SCL-1.

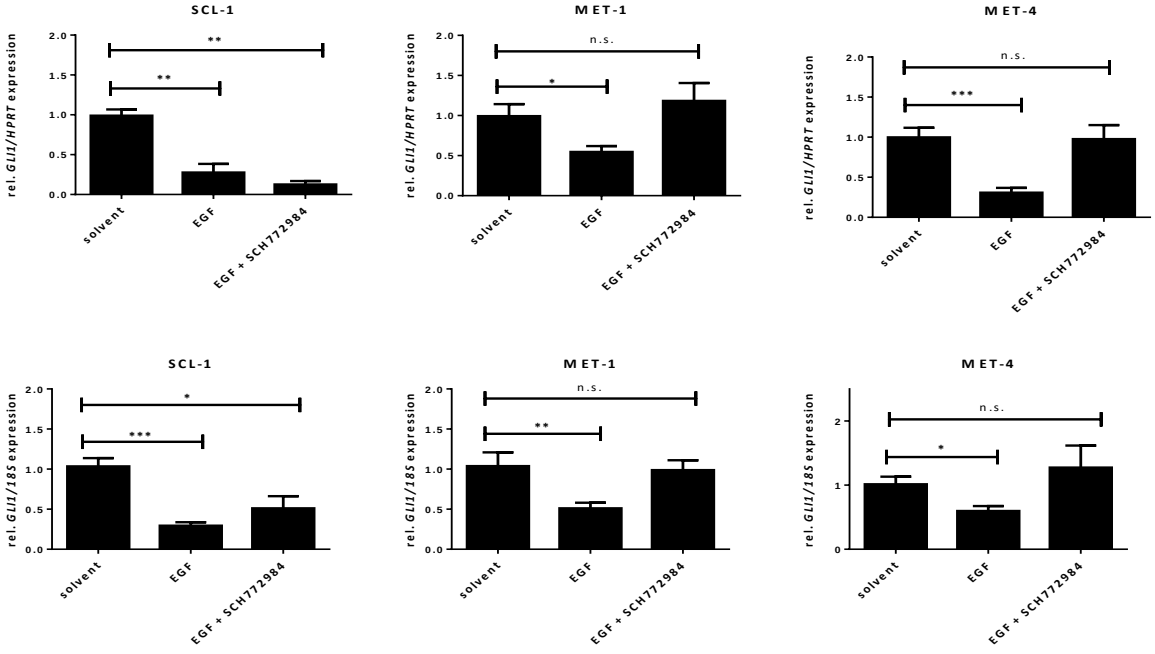

Figure 5: Effect of concomitant EGF treatment and ERK inhibition on *GLI1* expression level in cSCC cell lines. qRT-PCR representing *GLI1* expression upon treatment with 100 ng/µl EGF alone or EGF plus 0.1 µM SCH772984 for 24 h in SCL-1, MET-1 and MET-4 cells. The expression level was normalized to *HPRT* (upper panel) and *18S rRNA* (18S; lower panel). Gene expression data are shown as fold change to data of respective solvent-treated controls that were set to 1. Data are presented as mean values of three independent experiments measured in triplicates ± SEM; n.s., not significant; *, $p<0.05$; **, $p<0.01$; ***, $p<0.001$. Statistical comparisons were done with Mann-Whitney test.

In summary, EGF-induced *GLI1* downregulation is restored by ERK inhibition to basal level in MET-1 and MET-4 cell lines, but not in SCL-1 cells.

3.1.4 SCH772984 does not influence the proliferation of cSCC cells

To investigate the impact of SCH772984 on the proliferation of cSCC cell lines, BrdU assays were performed. However, there was no difference between SCH772984-treated and solvent-treated cells (Fig. 6), showing that ERK inhibition and related *GLI1* upregulation (see Fig. 4) do not affect proliferation of cSCC cell lines.

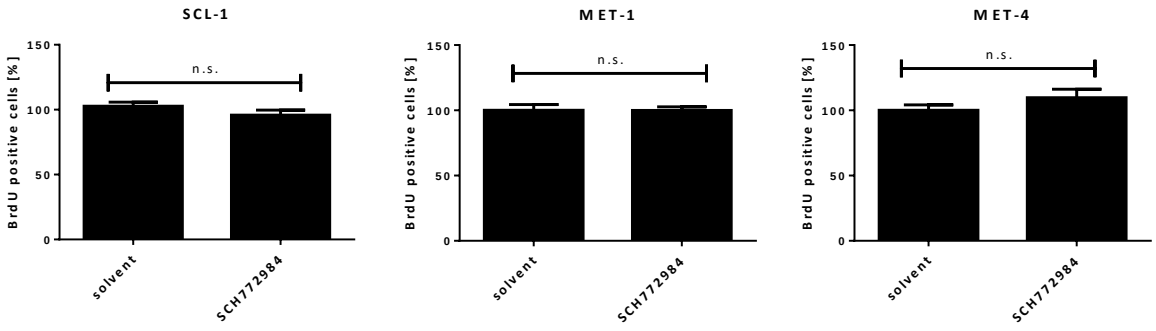

Figure 6: Impact of SCH772984 on the proliferation of SCL-1, MET-1 and MET-4 cell lines. BrdU incorporation assays showing the influence of 0.1 µM of SCH772984 on the proliferation of SCL-1, MET-1 and MET-4 cells after 24 h of incubation. The data are presented as the percentage of BrdU positive cells with the value of solvent-treated cells set to 100 %. Each graph represents the mean value ± SEM of three independent experiments; n.s., not significant. Statistical comparisons were done with Mann-Whitney test.

3.1.5 SCH772984 does not influence the metabolic activity of cSCC cells

In order to investigate if SCH772984 influences the metabolic activity of cSCC cell lines, WST-1 assays were performed. The cells were incubated with 0.1 µM of SCH772984 for 24 h and WST reagent was added for the last 3 h. Again, there was no difference in the metabolic activity between SCH772984- and solvent-treated samples (Fig. 7).

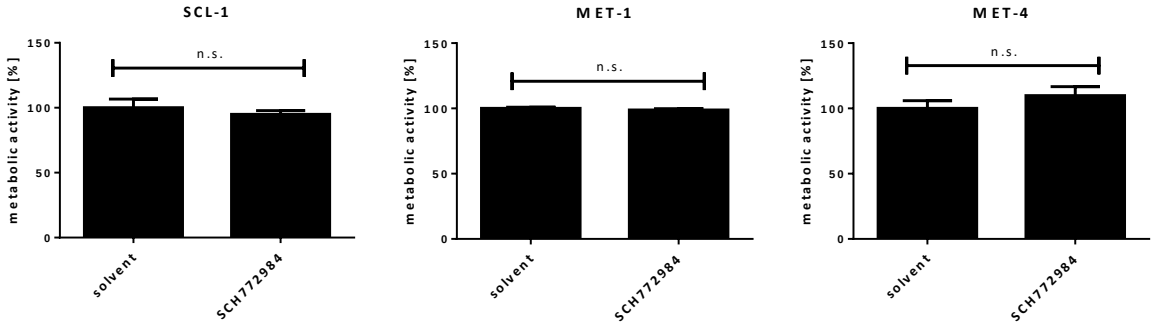

Figure 7: Impact of SCH772984 on the metabolic activity of SCL-1, MET-1 and MET-4 cell lines. WST-1 assays showing the influence of 0.1 µM of SCH772984 on the metabolic activity of SCL-1, MET-1 and MET-4 cells 24 h after incubation. The metabolic activity of the cells from the solvent-treated group was set to 100 %. Each graph represents the mean value ± SEM of three independent experiments; n.s., not significant. Statistical comparisons were done with Mann-Whitney test.

3.2 Role of EGF-mediated *GLI1* downregulation in migration and EMT of cSCC cells

Stainings of human cSCC samples performed in our working group suggested that *GLI1* was downregulated at the tumor invasion front. This observation led to the hypothesis that EGF-induced *GLI1* downregulation can lead to increased migratory capacity and EMT in cSCC cells. To test this hypothesis, the cells were treated with EGF or *GLI1*-specific siRNAs or were transfected with a GLI1-expressing plasmid. Cellular migration was measured by trans-well migration assay and EMT by gene expression analysis of the mesenchymal markers *ZEB1*, *ZEB2*, *TWIST*, *VIM*, *SNAIL* and of the epithelial marker *E-cadherin* (*CDH*).

The following experiments were mostly performed with the MET-4 cell line. This was due to the fact that SCL-1 cells did not show any migratory capacity and that the transfection method we used was too toxic for MET-1 cells.

3.2.1 Efficient *GLI1* knockdown in MET-4 cell line

First, we wanted to eliminate GLI1 function by using the GLI1/GLI2 inhibitor GANT61, which can inactivate GLI1 and GLI2. *GLI1* expression was used as a readout for GANT61 efficiency.

For the experiments, the cells were incubated with 10 µM and 30 µM of GANT61 for 24 h. According to the literature these concentrations are usually used when working with this inhibitor (Agyeman et al. 2014; Zhang et al. 2016). Unfortunately, GANT61 did not inhibit *GLI1* expression in any of the cSCC cell lines (Fig. 8A). However, it efficiently inhibited *GLI1* expression in the control cell line DAOY (Fig. 8B).

A

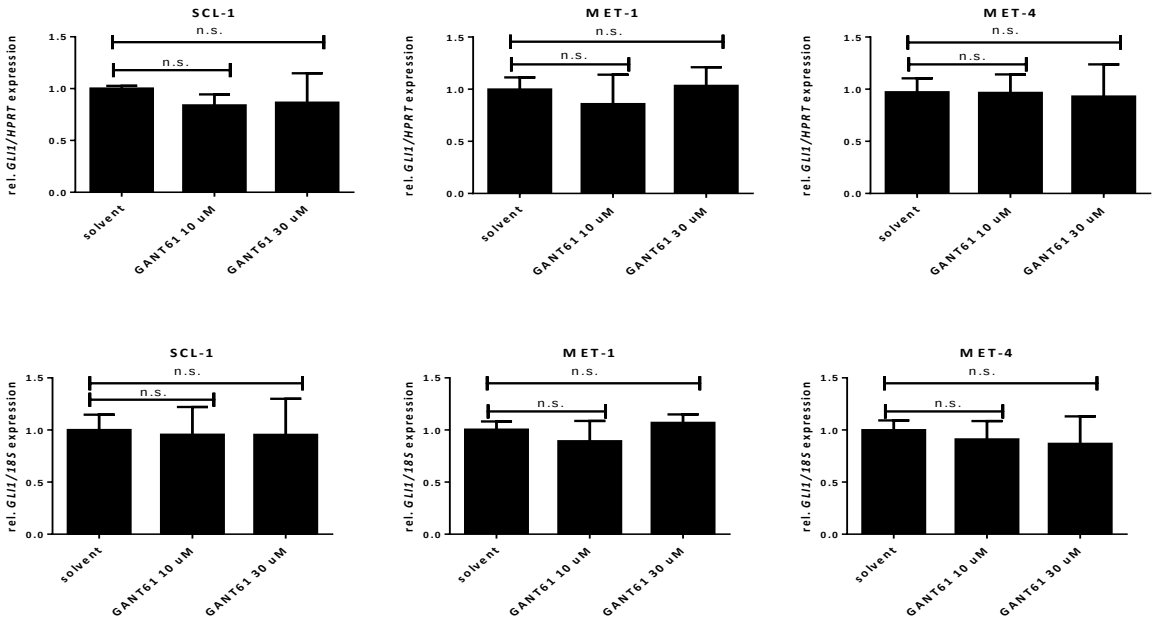

B

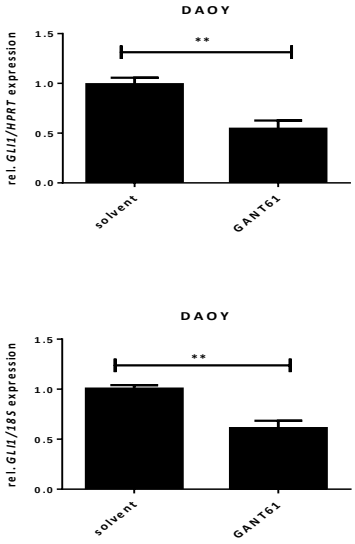

Figure 8: Effect of GANT61 on *GLI1* expression level in cSCC cell lines and the medulloblastoma cell line DAOY. **A)** qRT-PCR representing *GLI1* expression upon treatment with 10 µM or 30 µM GANT61 for 24 h in SCL-1, MET-1 and MET-4 cells. **B)** qRT-PCR representing *GLI1* expression upon treatment with 30 µM GANT61 for 24 h in DAOY cells. **A)** and **B)** The *GLI1* expression level was normalized to *HPRT* (upper panel) and *18S rRNA* (18S; lower panel). Gene expression data are shown as fold change to data of respective solvent treated controls that were set to 1. Data are presented as mean values of three independent experiments measured in triplicates ± SEM; n.s., not significant; **, $p<0.01$. Statistical comparisons were done with Mann-Whitney test.

These data show that GANT61 is not suitable to inhibit GLI1/GLI2 function in cSCC cells. Therefore, we used *GLI1* specific siRNA to knockdown *GLI1*. Cells were transfected for 24 h and 48 h with the siRNA and then mRNA was isolated and prepared for qRT-PCR. We not only measured *GLI1* but also *GLI2* since GLI2 is an endogenous target of GLI1. As shown in Figure 9 the *GLI1* specific siRNA significantly downregulates *GLI1* expression and even *GLI2* expression in MET-4 cells (Fig. 9). The expression data were normalized only against HPRT expression, as we observed that *18S rRNA* was regulated by the used siRNA pool.

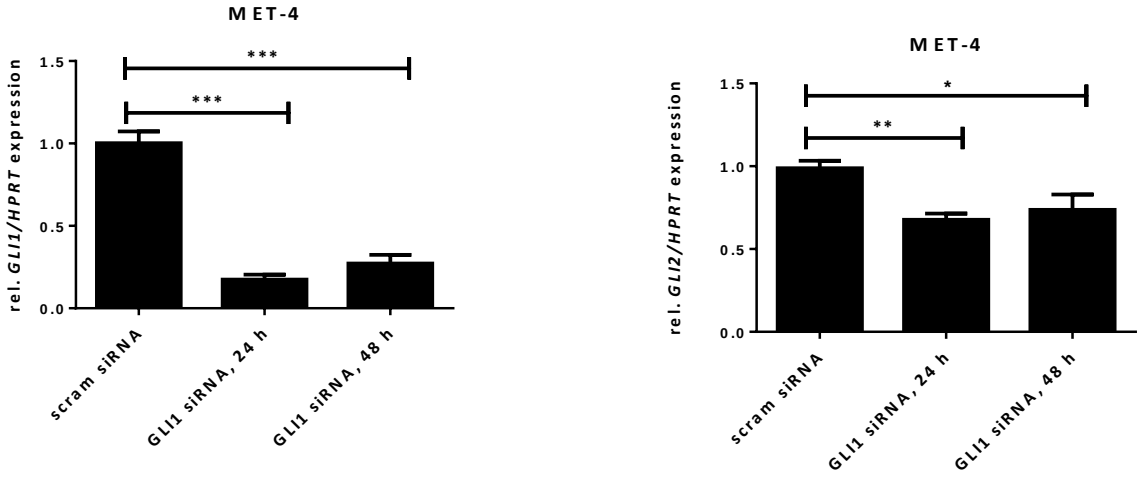

Figure 9: Effect of transfection with *GLI1* specific siRNA on GLI1 and GLI2 expression level in MET-4 cells. qRT-PCR representing *GLI1* and *GLI2* expression upon transfection with *GLI1* specific siRNA (GLI1 siRNA) in MET-4 cells. The expression level was normalized to *HPRT* gene expression and the values from control cells transfected with scrambled siRNA (scram siRNA) were set to 1. Data are presented as mean values of three independent experiments measured in triplicates ± SEM; *, $p<0.05$; **, $p<0.01$; ***, $p<0.001$. Statistical comparisons were done with Mann-Whitney test.

3.2.2 EGF treatment, as well as GLI1 knockdown, increased migratory capacity of MET-4 cells

To elucidate the role of EGF and related GLI1 downregulation in cSCC migration, MET-1 and MET-4 cells were first incubated with EGF. Whereas EGF did not significantly change the migratory capacity of MET-1 cells, incubation with EGF significantly increased the migratory capacity of MET-4 cells compared to solvent-treated samples (Fig. 10). The experiment was performed four times with MET-4 cells, but only two times with MET-1 cells and thus needs further validation.

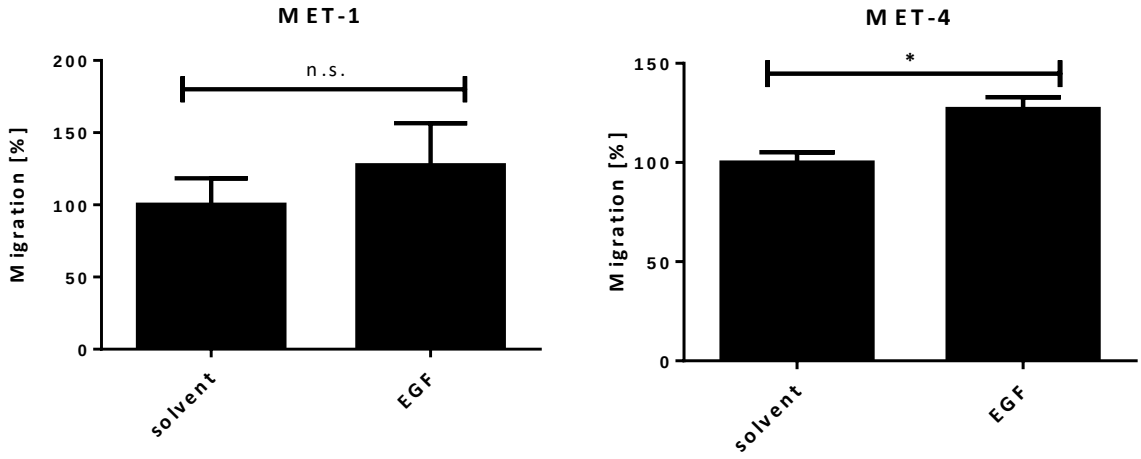

Figure 10: Effect of EGF on migratory capacity of MET-1 and MET-4 cells. Migratory capacity of the cells was measured by trans-well migration assay after 18 h incubation with 100 ng/µl EGF. The values from the solvent-incubated cells were set to 100 %. Each graph represents a summary of at least two independent experiments displayed as mean ± SEM; n.s., not significant; *, $p<0.05$. Statistical comparisons were done with Mann-Whitney test.

To investigate if GLI1 has any impact on the migratory capacity of cSCC cells, the migration assay was also performed after *GLI1* knockdown. Since we were unable to transfect MET-1 cells and since SCL-1 cells did not migrate at all, the experiment was only performed with MET-4 cells. As shown in Figure 11, the *GLI1* knockdown in MET-4 cells results in a significant increase in cell migration compared to control cells that have been transfected with scrambled siRNA (Fig. 11).

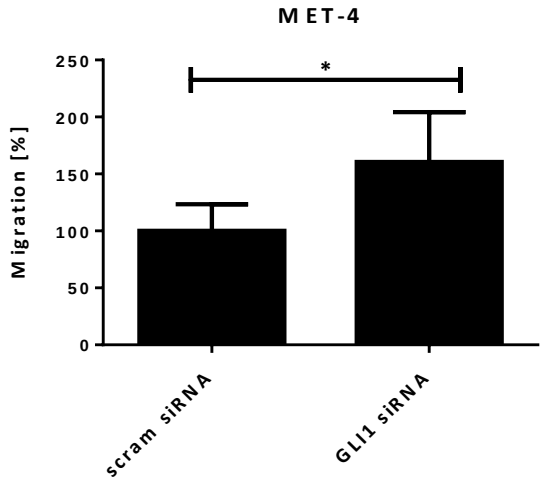

Figure 11: Influence of *GLI1* knockdown on the migratory capacity of MET-4 cells. Migratory capacity of the cells 24 h after transfection with GLI1 siRNA was measured by trans-well migration assay for 18 h. The value of MET-4 cells that have been transfected with scrambled siRNA (scram siRNA) was set to 100 %. Each graph represents a summary of three independent experiments displayed as mean ± SEM; *, $p<0.05$. Statistical comparisons were done with Mann-Whitney test.

To sum up, incubation with EGF as well as *GLI1* knockdown significantly increase the migratory capacity of MET-4 cells.

3.2.3 Effect of EGF treatment as well as *GLI1* knockdown on EMT

To investigate if the EGF-induced *GLI1* downregulation had any effect on EMT, the expression of the mesenchymal markers *ZEB1*, *ZEB2*, *TWIST*, *VIM*, *SNAIL* and of the epithelial marker *CDH* was measured. Whereas the mesenchymal markers are thought to be upregulated during EMT, the adhesion molecule *CDH* is generally downregulated.

In SCL-1 cells the mesenchymal markers *ZEB1*, *VIM* and *SNAIL* are upregulated after EGF treatment. However, the upregulation of *ZEB1* is only significant when the data are normalized to *18S mRNA*, but not when normalized to *HPRT*. Two other mesenchymal markers – *ZEB2* and *TWIST* - are on the contrary downregulated. This downregulation is significant when the data are normalized to *HPRT*, but not when normalized to *18S mRNA*. I also measured the expression of the epithelial marker *CDH*. However, in SCL-1, *CDH* was

not downregulated, but significantly upregulated when the data were normalized to *18S mRNA* (Fig. 12A)

In the MET-1 cell line *ZEB2* and *TWIST* were significantly downregulated in EGF-treated samples when normalized to *HPRT* expression. Similar tendencies were observed when the data were normalized to *18S mRNA* (Fig. 12B).

In MET-4, the expression of *ZEB1*, *ZEB2,* and *TWIST* was not significantly changed. *VIM* expression was not changed if normalized to *HPRT* but was significantly upregulated when normalized to *18S mRNA*. *SNAIL*, on the contrary, was significantly downregulated when normalized to *HPRT*, but not when normalized to *18S mRNA*. In contrast, *CDH* was significantly downregulated after EGF treatment when normalized to both housekeeper genes (Fig. 12C).

A

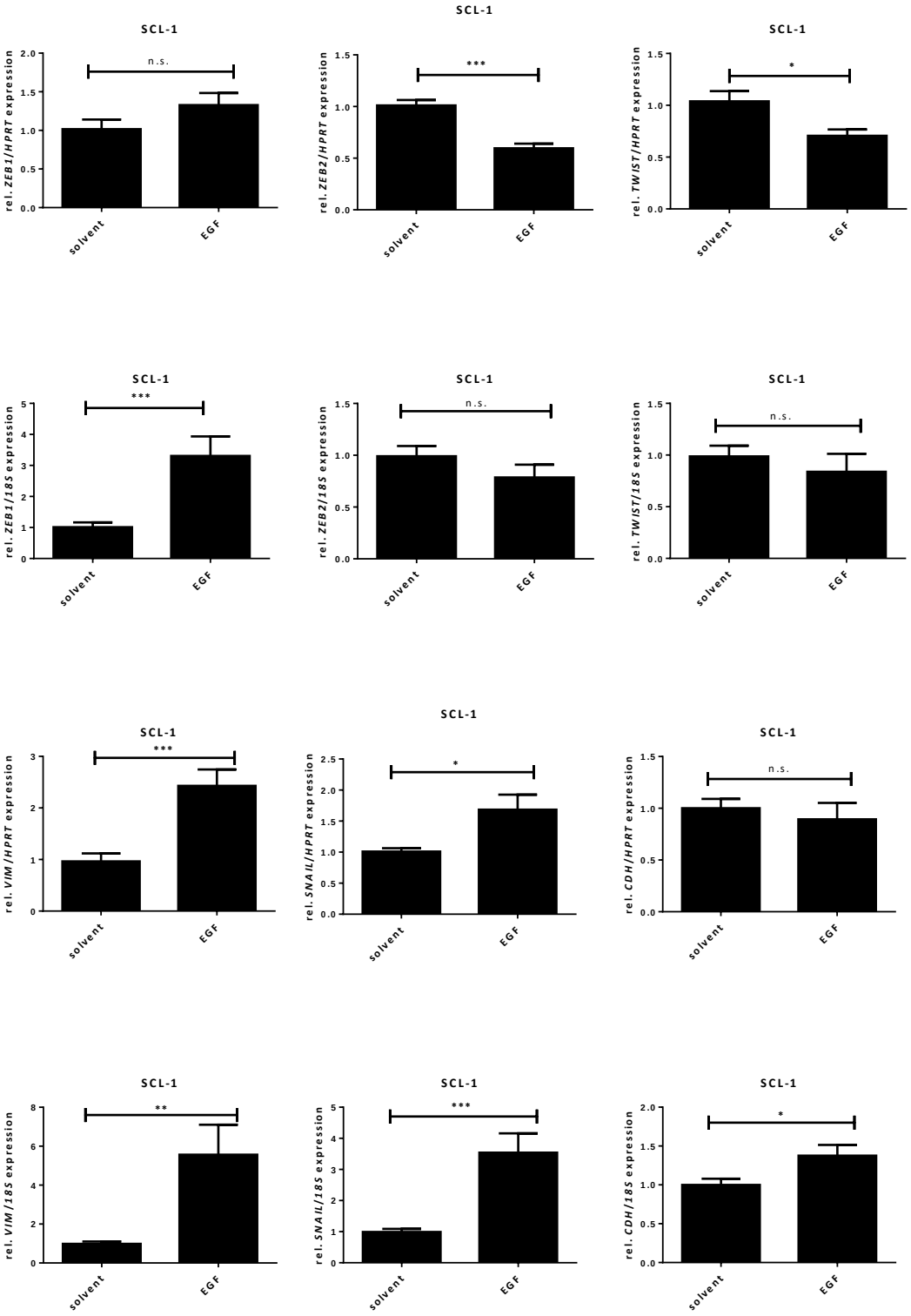
SCL-1
n.s.
rel. ZEB1/HPRT expression
SCL-1
***
rel. ZEB2/HPRT expression
SCL-1
*
rel. TWIST/HPRT expression
SCL-1
***
rel. ZEB1/18S expression
SCL-1
n.s.
rel. ZEB2/18S expression
SCL-1
n.s.
rel. TWIST/18S expression
SCL-1
***
rel. VIM/HPRT expression
SCL-1
*
rel. SNAIL/HPRT expression
SCL-1
n.s.
rel. CDH/HPRT expression
SCL-1
**
rel. VIM/18S expression
SCL-1
***
rel. SNAIL/18S expression
SCL-1
*
rel. CDH/18S expression
solvent
EGF

B

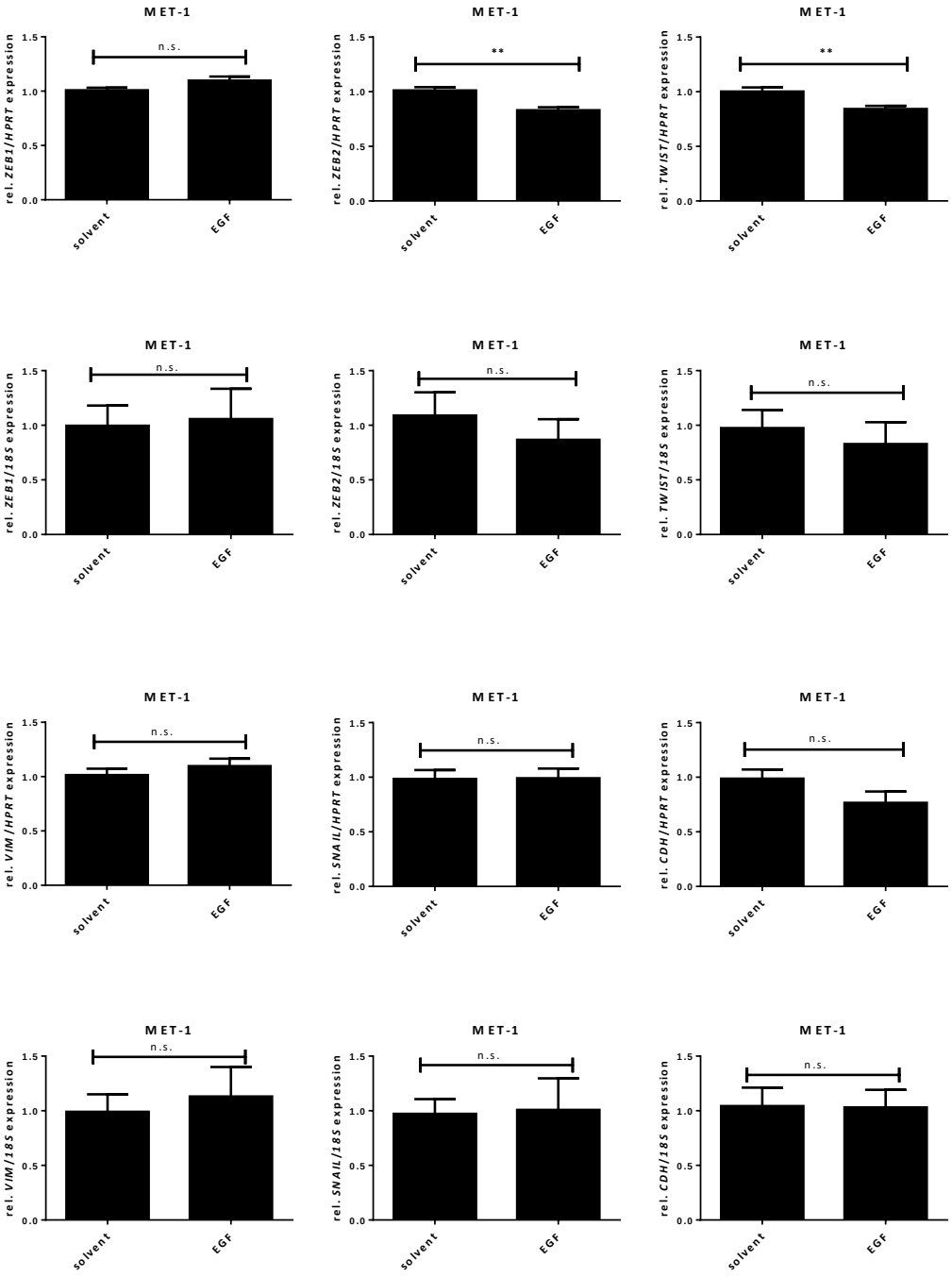
MET-1
n.s.
rel. ZEB1/HPRT expression
MET-1
**
rel. ZEB2/HPRT expression
MET-1
**
rel. TWIST/HPRT expression
MET-1
n.s.
rel. ZEB1/18S expression
MET-1
n.s.
rel. ZEB2/18S expression
MET-1
n.s.
rel. TWIST/18S expression
MET-1
n.s.
rel. VIM/HPRT expression
MET-1
n.s.
rel. SNAIL/HPRT expression
MET-1
n.s.
rel. CDH/HPRT expression
MET-1
n.s.
rel. VIM/18S expression
MET-1
n.s.
rel. SNAIL/18S expression
MET-1
n.s.
rel. CDH/18S expression
1.5
1.0
0.5
0.0
solvent
EGF

C

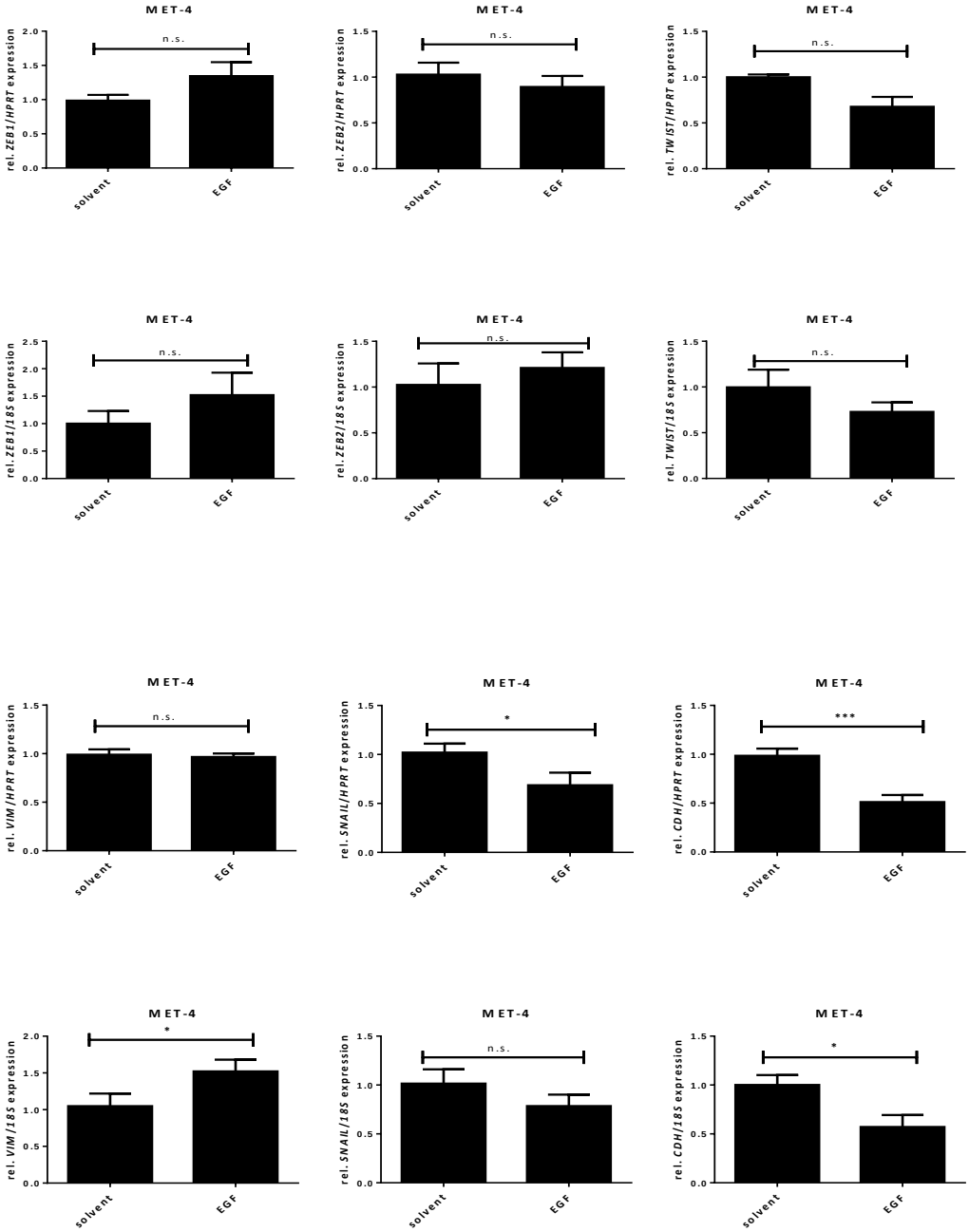

Figure 12: Expression of EMT markers after EGF treatment in SCL-1, MET-1 and MET-4 cell lines. qRT-PCR showing changes in *ZEB1*, *ZEB2*, *TWIST*, *VIM, SNAIL* and *CDH* expression level in SCL-1 **(A)**, MET-1 **(B)** and MET-4 **(C)** after treatment with 100 ng/µl EGF for 24 h in comparison to solvent treated cells. The gene expression was normalized to *HPRT* (upper panels) and *18S rRNA* (18S; lower panels) and data are shown as fold change to data of respective solvent treated controls that were set to 1. Each graph represents a summary of three independent experiments displayed as mean ± SEM; ns, not significant; *, $p<0.05$; **, $p<0.01$; ***, $p<0.001$; ****, $p<0.0001$. Statistical comparisons were done with Mann-Whitney test.

To sum up, the data are difficult to interpret, as EGF leads to the upregulation of some of the mesenchymal markers where others are rather downregulated. Another problem is the different results after normalization to either *HPRT* or *18S rRNA*. The only reliable conclusion that can be made is that EGF leads to the upregulation of *VIM* and *SNAIL* in SCL-1 and to downregulation of *CDH* in MET-4.

For studying the direct effect of *GLI1* downregulation on EMT, EMT markers were measured in *GLI1* knockdown cells after 24 h and 48 h of siRNA transfection. As we were unable to transfect MET-1 cell line with siRNA and since SCL-1 cells did not migrate, we focused on MET-4 cells. No changes were detected in *ZEB1* expression. *ZEB2* was not significantly downregulated after 24 h but significantly upregulated after 48 h. *TWIST* expression level was not changed after 24 h but was significantly downregulated after 48 h. *VIM* was also significantly downregulated at both time points, whereas no significant changes in *SNAIL* expression were observed. However, *CDH* was significantly downregulated after 24 h and the downregulation was even stronger after 48 h (Fig. 13).

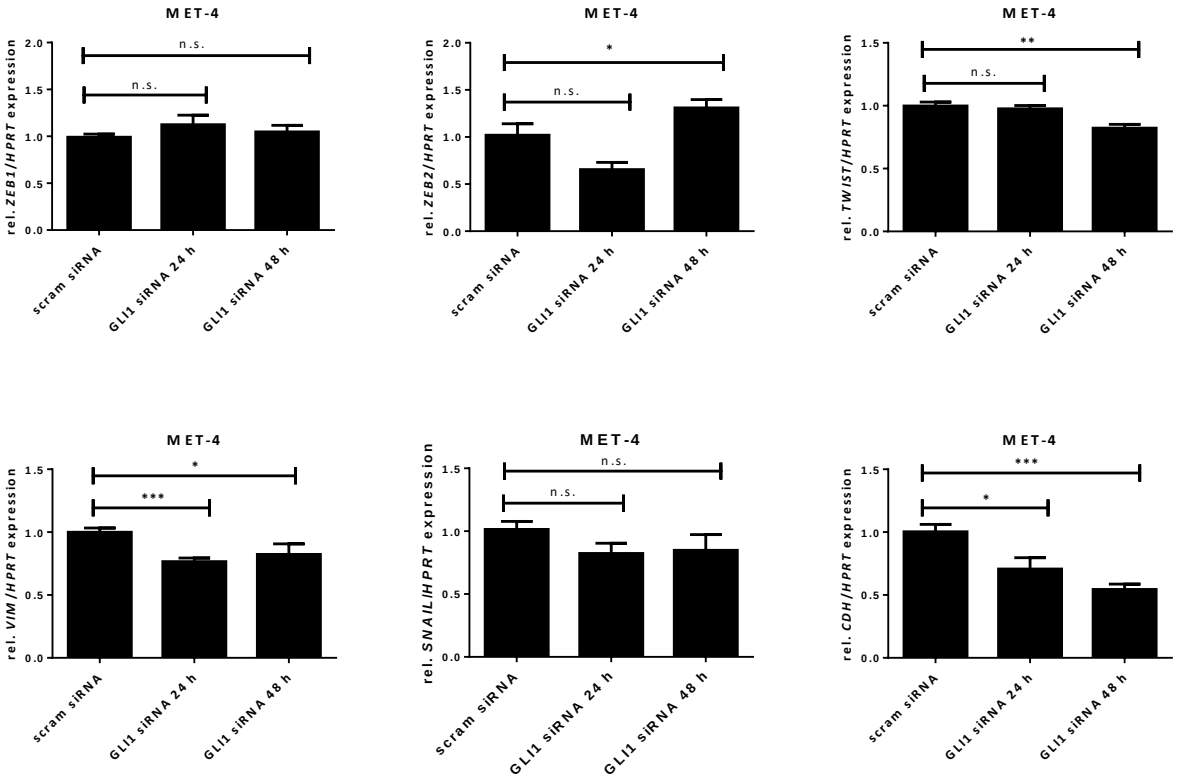

Figure 13: Effect of *GLI1* knockdown on the expression of EMT markers in MET-4 cell line. qPCR showing changes in *ZEB1*, *ZEB2*, *TWIST*, *VIM, SNAIL* and *CDH* expression level in MET-4 24 h and 48 h after transfection with *GLI1* specific siRNA. The expression level was normalized to *HPRT* gene expression. Data are shown as fold change to the control transfected with scrambled siRNA (scram siRNA) that was set to 1. Data are presented as mean values of two independent experiments measured in triplicates ± SEM; n.s., not significant; *, $p<0.05$; **, $p<0.01$; ***, $p<0.001$. Statistical comparisons were done with Mann-Whitney test.

In conclusion, a *GLI1* knockdown in MET-4 cells leads to the downregulation of the mesenchymal markers *TWIST* and *VIM*, but to upregulation of *ZEB2*. It also results in the downregulation of *CDH*, the only epithelial marker measured.

3.2.4 Efficient GLI1 overexpression in cSCC cell lines

To investigate the role of *GLI1* in migration and EMT of cSCC cells in more detail, the cells were also transfected with a plasmid encoding for GLI1. The level of *GLI1* and *GLI2* (as a downstream target of GLI1 protein) were assessed by qRT-PCR after mock transfection, transfection with an empty plasmid and with the plasmid expressing GLI1. As shown in Figure 12, the transfection leads to a significant increase of *GLI1* and *GLI2* expression in the SCL-1 and MET-4 cell lines (Fig. 14).

A

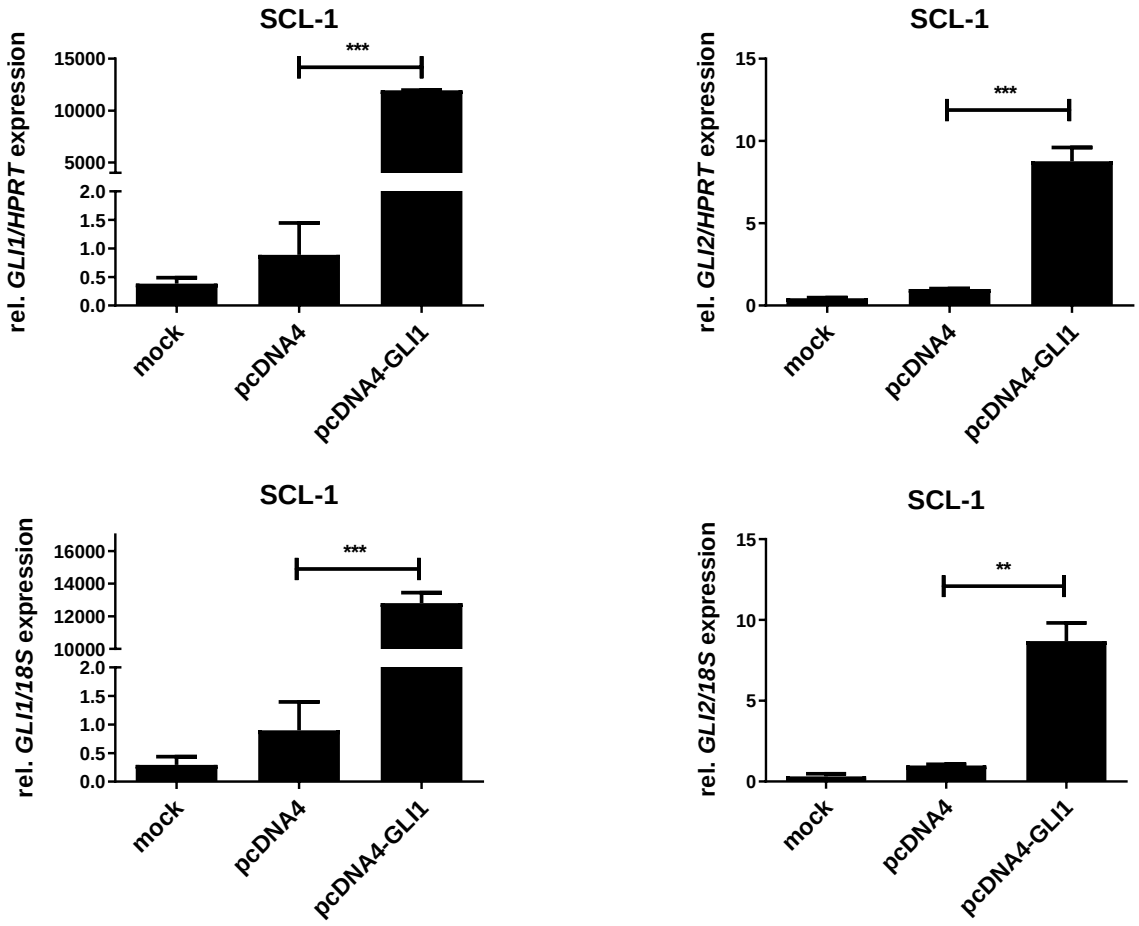

B

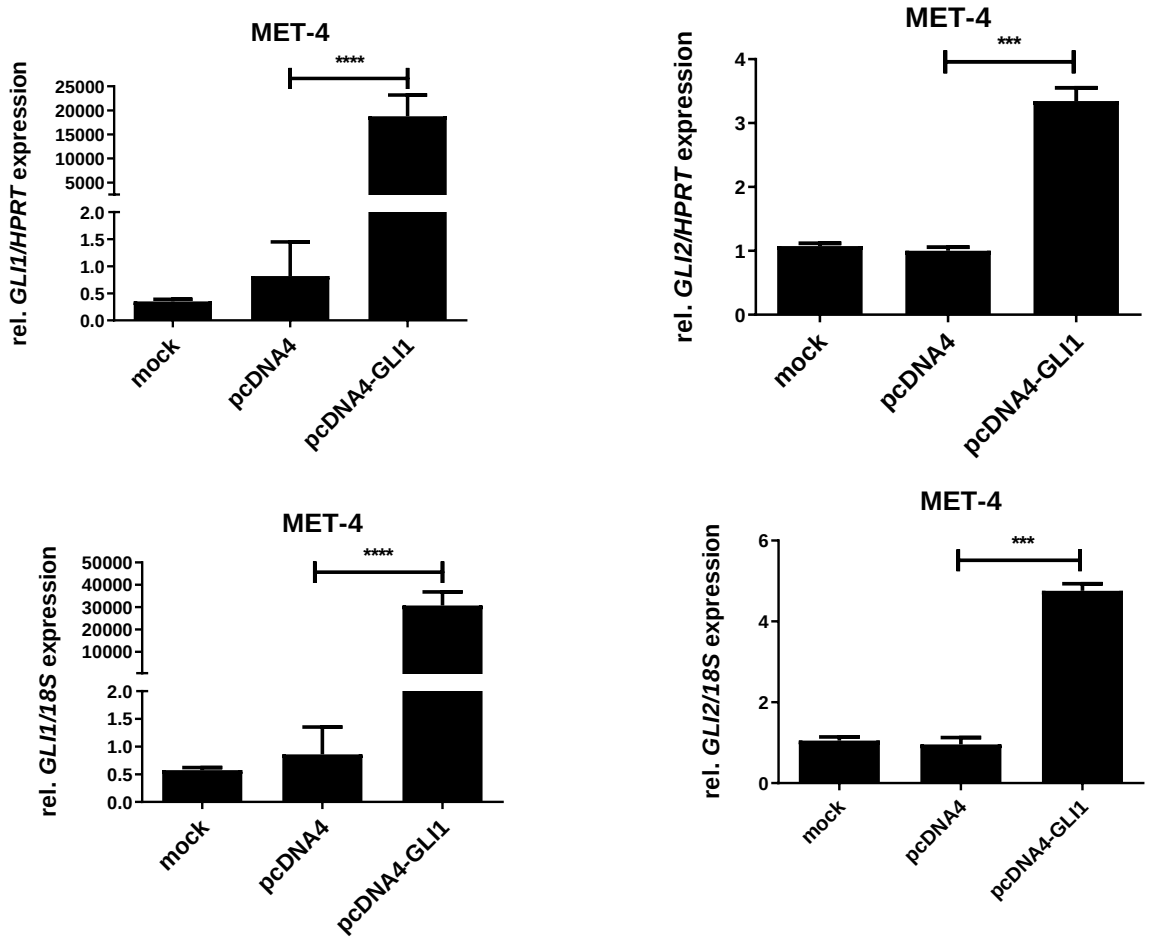

Figure 14: Effect of transfection with *GLI1* specific plasmid on *GLI1* and *GLI2* expression level. *GLI1* and *GLI2* expression level in SCL-1 **(A)** and MET-4 **(B)** cell lines as measured by qRT-PCR after transfection of the cells with a plasmid expressing *GLI1* (pcDNA4-GLI1) or pcDNA4 empty vector in comparison to mock-transfected cells. The data show relative expression levels normalized to *HPRT* (upper panel) and *18S rRNA* (18S; lower panel) in relation to the value of cells transfected with an empty vector, which was set to 1. Each graph represents a summary of three independent experiments displayed as mean ± SEM; ***, $p<0.001$; ****, $p<0.0001$. Statistical comparisons were done with Mann-Whitney test.

In conclusion, transfection with a plasmid expressing GLI1 results in significant upregulation of *GLI1* and *GLI2* in SCL-1 and MET-4 cells.

3.2.5 Effect of GLI1 overexpression on EMT

The expression of EMT markers was also measured after overexpression of GLI1 in SCL-1 and MET-4 cell lines. The results are shown in Figure 15 (Fig. 15A and 15B).

A

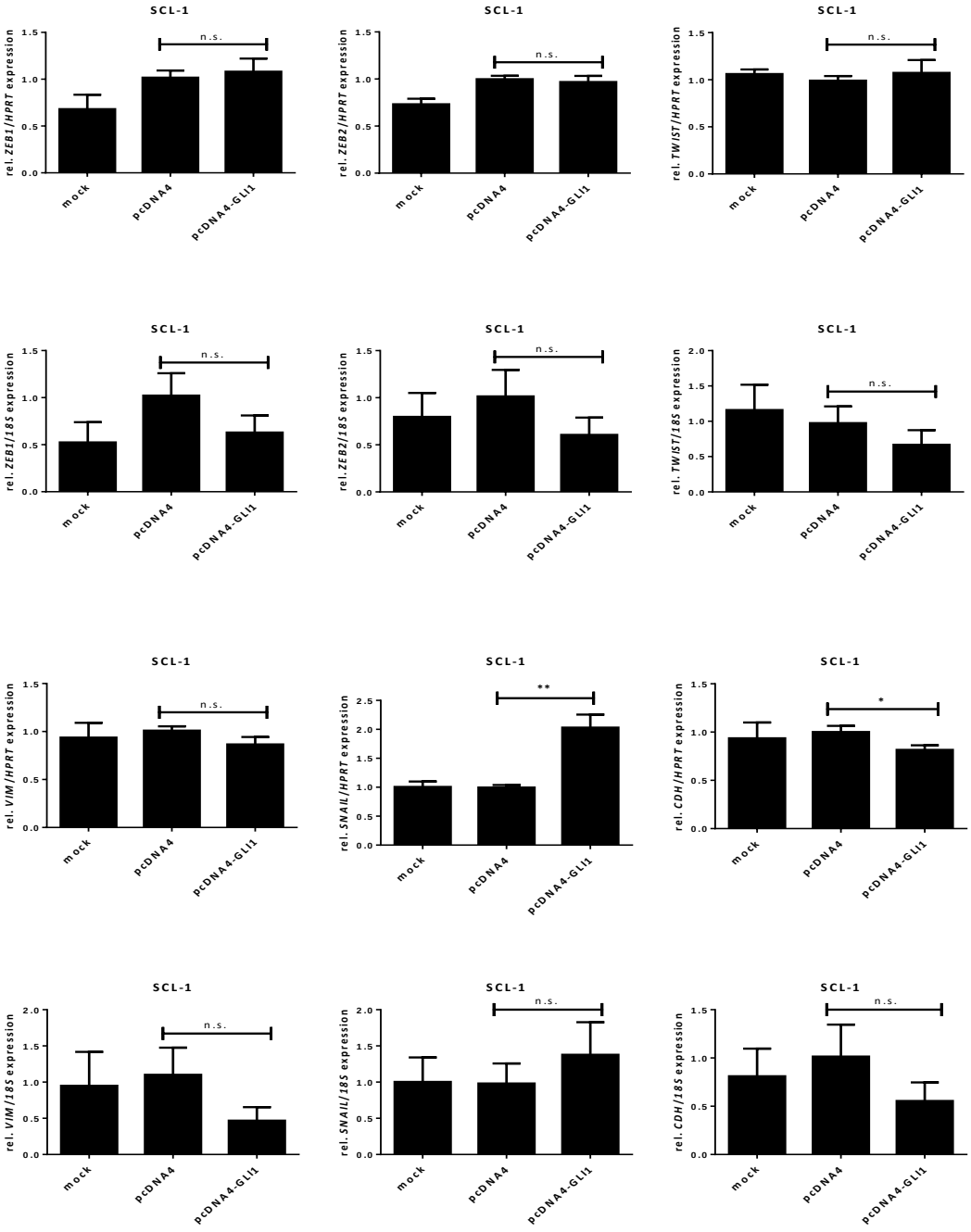

B

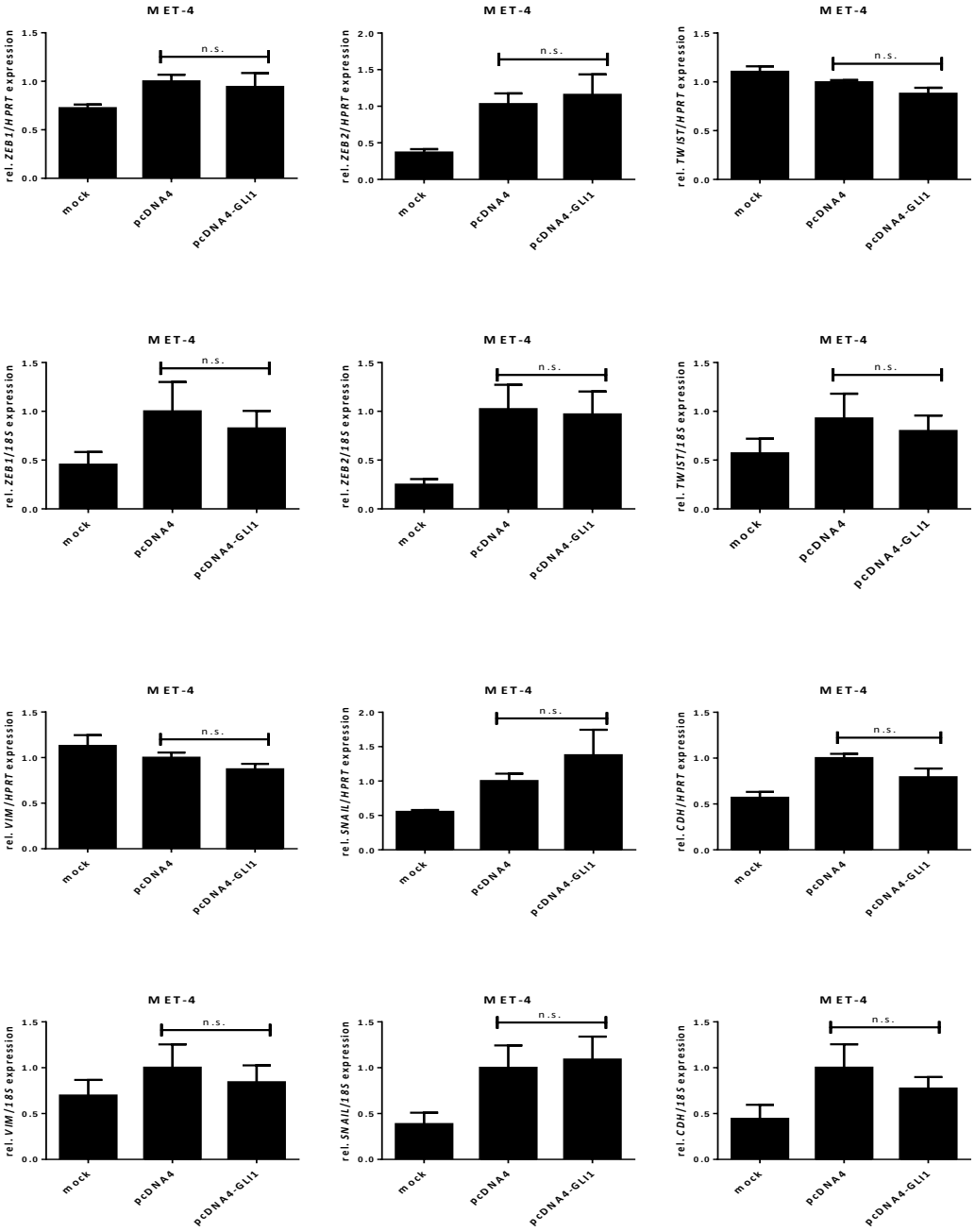

Figure 15: Expression of EMT markers after GLI1 overexpression in SCL-1 and MET-4 cell lines. qRT-PCR showing changes in *ZEB1*, *ZEB2*, *TWIST*, *VIM, SNAIL* and *CDH* expression level in SCL-1 **(A)** and in MET-4 **(B)** after transfection with a plasmid expressing GLI1 or pcDNA4 empty vector in comparison to mock-transfected cells. The data show relative expression levels normalized to *HPRT* (upper panels) and *18S rRNA* (lower panels) in relation to the value of cells transfected with an empty vector, which was set to 1. Each graph represents a summary of two independent experiments displayed as mean ± SEM; n.s., not significant; *, $p<0.05$; **, $p<0.01$. Statistical comparisons were done with Mann-Whitney test.

As shown in Figure 15A and 15B, the expression of the genes was not significantly changed in SCL-1 or MET-4 cells (Fig. 15A and 15B, respectively). The exceptions were *SNAIL* expression in SCL-1 cells that was significantly upregulated when normalized to *HPRT* and *CDH* expression in SCL-1 cells that was significantly downregulated when normalized to *HPRT*.

4 Discussion

4.1 EGF-induced downregulation of GLI1 via the MEK/ERK axis in cSCC

From previous experiments of the research group, it was known that the MEK1/2 inhibitor UO126 reversed the EGF-induced GLI1 downregulation in cSCC cell lines. Since the GLI1 levels in cells treated with EGF/UO126 went up to basal levels of solvent-treated cells (Pyczek 2018), we assumed that the EGF-induced GLI1 downregulation is mediated via MEK or by one of its downstream molecules, like ERK.

To elucidate the mechanism of GLI1 downregulation, we used SCH772984 that inhibits ERK1/2. Indeed, we found that treatment with SCH772984 reversed EGF-induced GLI1 downregulation in MET-1 and MET-4 cell lines. However, in SCL-1 cells this was not the case. This indicates that in MET-1 and MET-4, GLI1 inhibition is mediated via ERK1/2, while in SCL-1 GLI1 is inhibited by MEK1/2. Based on these results, our current model is represented in Figure 16.

Until recently, ERK1/2 was thought to be the only biological substrate of MEK1/2, but lately, HSF1 that is involved in proteotoxic stress response was also reported to be regulated directly by MEK1/2 (Tang et al. 2015). To our knowledge, no other MEK1/2 substrates have been described in the literature. HSF1 is known to activate heat shock protein HSP90 (Dai et al. 2007), and HSP90 induces resorption of primary cilia that is correlated with a reduction in HH signaling (Prodromou et al. 2012). Thus, MEK1/2 inhibition could be followed by the inactivation of HSF1 and HSP90, which may result in cilia formation. This could allow for the activation of canonical HH signaling activity back to normal levels. If this is true, SCL-1 cells should secrete an HH ligand. Since the production of SHH was ruled out in SCL-1 by previous experiments of our lab (Pyczek 2018), one should now also check for the production of IHH or DHH.

In contrast to MEK1/2, there are numerous substrates of ERK1/2, including the transcription factors Ets, Elk, c-Fos (Roskoski 2012) and also GLI1. Thus, direct

phosphorylation and thus activation of GLI1 by ERK1 has been described in lung adenocarcinoma (Po et al. 2017). However, in our setting in MET-1 and MET-4 cells, ERK1/2 should inhibit GLI transcription factors and thus GLI1 expression. Indeed, there is a report that describes that FGF counteracts HH/GLI-dependent proliferation and growth of medulloblastoma, which is mediated, at least in part, by activation of ERK (Fogarty MP et al. 2007). Furthermore, in medulloblastoma, the ERK1/2 substrates MEKK2 (MAP3K2) and MEKK3 (MAP3K3) inhibit GLI1 transcriptional activity and oncogenic function through phosphorylation on multiple Ser/Thr sites of GLI1, which reduces GLI1 protein stability, DNA-binding ability, and increases the association of GLI1 with SUFU (Lu et al. 2018). There are also several other ways how *GLI1* transcription could be negatively regulated via MEK/ERK axis. One possibility is inhibition of activator GLI2/3 forms, while another option is the stabilization of GLI2/3 repressor forms. It is also possible that MEK/ERK inhibit translocation of the GLI activator forms into the nucleus.

It finally remains to be investigated if the downregulation of *GLI1*-transcription corresponds with inhibition of GLI1 on the protein level. It should be taken into account that protein regulation takes more time than the regulation of mRNA.

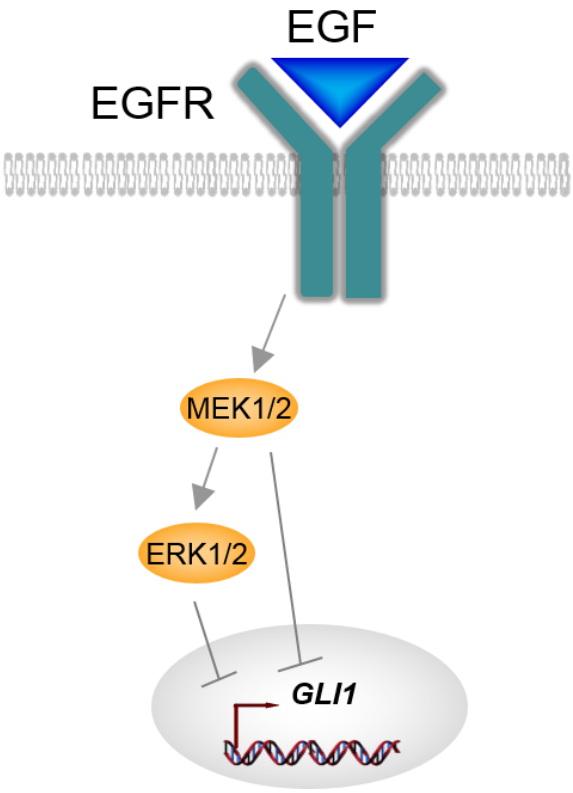

Figure 16: Simplified schematic diagram of EGF-induced GLI1 downregulation via the MEK/EKR axis in cSCC. EGF leads to activation of MEK1/2 that inhibits GLI1 expression in the SCL-1 cell line while in MET-1 and MET-4 cell lines GLI1 inhibition is mediated via ERK1/2. The downstream events of MEK1/2 or ERK1/2, which mediate inhibition of *GLI1* transcription are unknown.

In this study, only three cSCC cell lines were used. As the cell lines MET-1 and MET-4 both are derived from the same patient, it is difficult to judge whether GLI1 inhibition by ERK is the dominant mechanism or if it is present only in the small group of cSCC. To answer this question, one could perform immunohistochemistry of human tissue samples using antibodies against phosphorylated MEK and ERK and could try to correlate their expression with that of GLI1. The latter staining should be done by in-situ-hybridization because our lab is not aware of an anti-GLI1-antibody that reveals good and reliable results on human tissue.

The literature about GLI1 regulation by EGF in cancer is very sparse. Po et al. have shown that in lung adenocarcinoma EGF promotes GLI1 activation and concomitantly growth of tumor *in vivo* (Po et al. 2017). In medulloblastoma FGF/FGFR-mediated activation of

ERK has been observed and – as already stated above – activation of ERK results in inhibition of HH signaling pathway target genes, including *GLI1* (Fogarty MP et al. 2007). A negative correlation between GLI1 and EGF levels has also been observed by Keysar et al in head and neck SCC (HNSCC), in which EGFR signaling downregulates GLI1 in EGFR-dependent HNSCC (Keysar et al. 2013). In the same publication, the authors also described that inhibition of GLI1, on the other hand, increased EGFR dependency of the tumors and enhanced anti-EGFR therapy efficacy. These results suggest that combination treatment with e.g. the EGFR-binding monoclonal antibody Cetuximab and a GLI1-inhibitor may intensify the antitumoral effect.

Our experiments also showed that SCH772984 had no effect on proliferation and on metabolic activity. This was excluded via BrdU and WST assays, respectively. This was surprising because ERK has been reported to promote cell proliferation in many different types of cancer e.g. pancreatic and hepatocellular carcinoma (Chen et al. 2016) and that accordingly, SCH772094 inhibits proliferation of pancreatic cancer cells and also of BRAF- or MEK-inhibitor resistant melanoma (Morris et al. 2013; Zhou et al. 2017). However, the lack of any antiproliferative effect of SCH772984 in cSCC cells could be due to circumstance that the proliferation of cSCC cells is not mediated by ERK1/2 or by GLI1.

4.2 The effects of GLI1 downregulation and GLI1 overexpression on migration and EMT of cSCC

In this thesis, the migration of cSCC cell lines was studied by insert migration assay. Another method to assess cellular migration is scratch assay. However, the disadvantage of this method is the difficulty to eliminate the effects of proliferation. Thus, when cells fill the gap, one cannot judge if this is due to migration or simply due to proliferation. Indeed, all three cSCC cell lines strongly proliferated and it was impossible to inhibit proliferation by culturing cells even in starvation medium containing 0.5 % FCS.

The data of the insert migration assay show that both EGF-treatment and *GLI1* knockdown can lead to an increased migratory capability of cSCC cells. However, EGF-treatment

significantly increased the migration of MET-4, but not of MET-1 cells. Since the experiments were performed only two times, additional experiments are needed to validate these results. The increase of cellular migratory capability by EGF has been observed in many tumor entities, for example in esophageal squamous cell carcinoma and adenocarcinoma cells (Fichter et al. 2014), in which migration was reduced upon treatment with TKIs. Interestingly, similarly to EGF treatment, the *GLI1* knockdown in MET-4 cells also increased the migratory capability, suggesting that GLI1 normally inhibits the migration of cSCC cells.

This was surprising because the effect of GLI1 on migration is different in other tumor entities. Thus, in non-small cell lung cancer, cervix cancer, and osteosarcoma, GLI1 promotes migration (Wang et al. 2018; Yang et al. 2018; Yu et al. 2018). This is also seen in BCC (Bakry et al. 2015). The contrasting effect of GLI1 on cell migration in cSCC can be explained by a very distinct role of HH signaling in cSCC. It is also possible that the inhibitory effect of GLI1 on migration is an individual characteristic of MET-4 cells. The use of additional cSCC cell lines could help to answer this question.

Even though there are data showing that migration is not necessarily coupled with EMT (Schaeffer et al. 2014), we tried to assess EMT by measurement of EMT markers, which are usually used for this purpose (see e.g. (Keysar et al. 2013)). EGF-induced EMT has been observed in different cancer entities, including hepatocellular carcinoma and oral squamous cell carcinoma (Fujiwara et al. 2018; Lim et al. 2019). Pan et al. (2018) have seen that EGF-induced EMT is mediated via ERK1/2 in HNSCC. Keysar et al. (2013) observed that EGF increased cellular motility and induced an EMT-like phenotype in HNSCC by significantly upregulating the mesenchymal markers *ZEB1* and *VIM*. In contrast, our results were very heterogeneous. Varying results were observed when different housekeepers were used for normalization. The housekeepers that we used were *18S* rRNA and *HPRT*. The divergent results may be due to the regulation of one of the housekeepers under the respective experimental settings. In addition, it is possible that the measurement of *18S* rRNA is somewhat imprecise. Thus, *18S* rRNA is a very abundant cellular RNA, which requires several steps of serial dilutions until the amount is suitable for use in qRT-PCR. To solve this problem one could employ a third housekeeper to find out if there are two housekeeper

genes leading to similar results when used for normalization. In addition, one could assess the expression of the EMT markers by Western Blot or by immunohistochemistry.

Another possibility to reveal more reliable results may be to culture the cSCC cells in 3D culture models such as spheroids, as they better mimic the *in vivo* tumor microenvironment. Indeed, HNSCC cells grown as spheroid cultures showed mesenchymal-like characteristics and expressed GLI1 at higher levels than under normal culture conditions, i.e. 2D culture conditions (Essid et al. 2018). In a follow-up experiment, Melissaridou et al. (2019) compared the effects of the 2D and 3D cell cultures on the EMT profile of HNSCC. They observed that the expression of CDH1 and SOX2 is consistently upregulated in spheroids of all cell lines when compared to the respective 2D monolayers, whereas the expression of EGFR and other EMT markers such as Vimentin and N-cadherin strongly varied between the cell lines. Thus, it is possible that the gene expression profile of cSCC cells behaves similar to that observed by Melissaridou et al. and that the cSCC cells may express CDH1 and SOX2 when cultured as spheroids. However, this is pure speculation and remains to be validated in the future.

5 Summary

Cutaneous squamous cell carcinoma (cSCC) is the second most common non-melanoma skin cancer and its incidence is increasing worldwide. This highlights the importance of a better understanding of the molecular mechanisms of cSCC to improve the current treatment strategies. Both, epidermal growth factor receptor (EGFR)-signaling and Hedgehog (HH) signaling, are involved in cSCC.

In this thesis, we tried to investigate the role of HH signaling and its interaction with the EGFR-pathway in cSCC. The activity of HH signaling was assessed based on the mRNA expression of its main target GLI1. Since previous studies from our research group revealed that EGF treatment downregulates *GLI* expression via MEK, we used the specific ERK1/2 inhibitor SCH772984 to investigate if the downregulation is mediated downstream of MEK via ERK. The data revealed that EGF-induced *GLI1* downregulation is restored to basal level by ERK inhibition in MET-1 and MET-4 cell lines, but not in SCL-1 cells. These results suggest that the observed EGF-induced *GLI1* downregulation is mediated via ERK in MET-1 and MET-4 cells, but via MEK in SCL-1 cell line. We also observed that ERK inhibition does not alter the proliferation or metabolic activity of the investigated cell lines.

In the next part of this thesis, we focused on the role of HH signaling in migration and epithelial-to-mesenchymal transition (EMT) of cSCC. For this purpose, we analyzed EGF-treated cells or cells in which GLI1 was knocked down or was overexpressed.

Migration was measured by insert migration assay. Because SCL-1 cells did not show any migratory capacity, we focused on MET-1 and MET-4 cell lines. The data revealed that EGF-treatment, as well as a GLI1-knockdown, increased the migratory capacity of MET-4 cells. However, these experiments should be repeated since they were performed only twice. Unfortunately, we were unable to transfect MET-1 with *GLI1* targeting siRNA.

We also tried to investigate the impact of GLI1 on EMT by analyzing the expression of the mesenchymal markers *ZEB1*, *ZEB2*, *TWIST*, *VIM*, *SNAIL* and the epithelial marker *E-cadherin* (*CDH*). The expression of EMT-markers was measured in EGF-treated cells and in cells in which GLI1 was knocked-down or as overexpressed. However, different results were obtained when normalizing the gene expression data to different housekeeper genes.

Therefore, the current data are difficult to interpret, and additional investigations are needed to specify the results.

6 References

Agyeman A, Jha BK, Mazumdar T, Houghton JA (2014): Mode and specificity of binding of the small molecule GANT61 to GLI determines inhibition of GLI-DNA binding. Oncotarget 5

Alam M, Ratner D (2001): Cutaneous Squamous-Cell Carcinoma. N Engl J Med 344, 975–983

Anjum R, Blenis J (2008): The RSK family of kinases: emerging roles in cellular signalling. Nat Rev Mol Cell Biol 9, 747–758

Arron ST, Graham Ruby J, Dybbro E, Ganem D, DeRisi JL (2011): Transcriptome Sequencing Demonstrates that Human Papillomavirus Is Not Active in Cutaneous Squamous Cell Carcinoma. J Invest Dermatol 131, 1745–1753

Azuma M, Danenberg KD, Iqbal S, El-Khoueiry A, Zhang W, Yang D, Koizumi W, Saigenji K, Danenberg PV, Lenz H-J (2006): Epidermal growth factor receptor and epidermal growth factor receptor variant III gene expression in metastatic colorectal cancer. Clin Colorectal Cancer 6, 214–218

Bakry OA, Samaka RM, Shoeib MAM, Megahed DM (2015): Immunolocalization of Glioma-Associated Oncogene Homolog 1 in Non Melanoma Skin Cancer. Ultrastruct Pathol 39, 135–146

Barnes EA, Kong M, Ollendorff V, Donoghue DJ (2001): Patched1 interacts with cyclin B1 to regulate cell cycle progression. EMBO J 20, 2214–2223

Bates RC, Bellovin DI, Brown C, Maynard E, Wu B, Kawakatsu H, Sheppard D, Oettgen P, Mercurio AM (2005): Transcriptional activation of integrin beta6 during the epithelial-mesenchymal transition defines a novel prognostic indicator of aggressive colon carcinoma. J Clin Invest 115, 339–347

Belgacem YH, Borodinsky LN (2011): Sonic hedgehog signaling is decoded by calcium spike activity in the developing spinal cord. Proc Natl Acad Sci U S A 108, 4482–4487

Bhutani T, Abrouk M, Sima CS, Sadetsky N, Hou J, Caro I, Chren M-M, Arron ST (2017): Risk of cutaneous squamous cell carcinoma after treatment of basal cell carcinoma with vismodegib. J Am Acad Dermatol 77, 713–718

Bikle DD, Oda Y, Xie Z (2004): Calcium and 1,25(OH)2D: interacting drivers of epidermal differentiation. J Steroid Biochem Mol Biol 89–90, 355–360

Bitgood MJ, Shen L, McMahon AP (1996): Sertoli cell signaling by Desert hedgehog regulates the male germline. Curr Biol CB 6, 298–304

Bondzi C, Grant S, Krystal GW (2000): A novel assay for the measurement of Raf-1 kinase activity. Oncogene 19, 5030–5033

Boriack-Sjodin PA, Margarit SM, Bar-Sagi D, Kuriyan J (1998): The structural basis of the activation of Ras by Sos. Nature 394, 337–343

Boukamp P, Tilgen W, Dzarlieva RT, Breitkreutz D, Haag D, Riehl RK, Bohnert A, Fusenig NE (1982): Phenotypic and genotypic characteristics of a cell line from a squamous cell carcinoma of human skin. J Natl Cancer Inst 68, 415–427

Briscoe J, Chen Y, Jessell TM, Struhl G (2001): A Hedgehog-Insensitive Form of Patched Provides Evidence for Direct Long-Range Morphogen Activity of Sonic Hedgehog in the Neural Tube. Mol Cell 7, 1279–1291

Brodland DG, Zitelli JA (1992): Surgical margins for excision of primary cutaneous squamous cell carcinoma. J Am Acad Dermatol 27, 241–248

Brtva TR, Drugan JK, Ghosh S, Terrell RS, Campbell-Burk S, Bell RM, Der CJ (1995): Two distinct Raf domains mediate interaction with Ras. J Biol Chem 270, 9809–9812

Buday L, Downward J (1993): Epidermal growth factor regulates p21ras through the formation of a complex of receptor, Grb2 adapter protein, and Sos nucleotide exchange factor. Cell 73, 611–620

Buglino JA, Resh MD (2008): Hhat is a palmitoylacyltransferase with specificity for N-palmitoylation of Sonic Hedgehog. J Biol Chem 283, 22076–22088

Burke R, Nellen D, Bellotto M, Hafen E, Senti KA, Dickson BJ, Basler K (1999): Dispatched, a novel sterol-sensing domain protein dedicated to the release of cholesterol-modified hedgehog from signaling cells. Cell 99, 803–815

Cañueto J, Cardeñoso E, García JL, Santos-Briz Á, Castellanos-Martín A, Fernández-López E, Blanco Gómez A, Pérez-Losada J, Román-Curto C (2017): Epidermal growth factor receptor expression is associated with poor outcome in cutaneous squamous cell carcinoma. Br J Dermatol 176, 1279–1287

Capiod T, Shuba Y, Skryma R, Prevarskaya N (2007): Calcium signalling and cancer cell growth. Subcell Biochem 45, 405–427

Carpenter G, Lembach KJ, Morrison MM, Cohen S (1975): Characterization of the binding of 125-I-labeled epidermal growth factor to human fibroblasts. J Biol Chem 250, 4297–4304

Ceresa BP, Peterson JL: Chapter Five - Cell and Molecular Biology of Epidermal Growth Factor Receptor. In: Jeon KW (Hrsg.): International Review of Cell and Molecular Biology. Band 313; Academic Press 2014, 145–178

Chen JK, Taipale J, Young KE, Maiti T, Beachy PA (2002): Small molecule modulation of Smoothened activity. Proc Natl Acad Sci U S A 99, 14071–14076

Chen X, Tukachinsky H, Huang C-H, Jao C, Chu Y-R, Tang H-Y, Mueller B, Schulman S, Rapoport TA, Salic A (2011): Processing and turnover of the Hedgehog protein in the endoplasmic reticulum. J Cell Biol 192, 825–838

Chen Y, Liu Q, Wu M, Li M, Ding H, Shan X, Liu J, Tao T, Ni R, Chen X (2016): GAB2 promotes cell proliferation by activating the ERK signaling pathway in hepatocellular carcinoma. Tumor Biol 37, 11763–11773

Chiang C, Litingtung Y, Lee E, Young KE, Corden JL, Westphal H, Beachy PA (1996): Cyclopia and defective axial patterning in mice lacking Sonic hedgehog gene function. Nature 383, 407–413

Chipperfield MP, Dhomse SS, Feng W, McKenzie RL, Velders GJM, Pyle JA (2015): Quantifying the ozone and ultraviolet benefits already achieved by the Montreal Protocol. Nat Commun 6, 7233

Chuang P-T, McMahon AP (1999): Vertebrate Hedgehog signalling modulated by induction of a Hedgehog-binding protein. Nature 397, 617–621

Cohen S (1962): Isolation of a mouse submaxillary gland protein accelerating incisor eruption and eyelid opening in the new-born animal. J Biol Chem 237, 1555–1562

Cooper MK, Porter JA, Young KE, Beachy PA (1998): Teratogen-mediated inhibition of target tissue response to Shh signaling. Science 280, 1603–1607

Cunningham MP, Essapen S, Thomas H, Green M, Lovell DP, Topham C, Marks C, Modjtahedi H (2005): Coexpression, prognostic significance and predictive value of EGFR, EGFRvIII and phosphorylated EGFR in colorectal cancer. Int J Oncol 27, 317–325

Dai C, Whitesell L, Rogers AB, Lindquist S (2007): Heat Shock Factor 1 Is a Powerful Multifaceted Modifier of Carcinogenesis. Cell 130, 1005–1018

Danaee H, Karagas MR, Kelsey KT, Perry AE, Nelson HH (2006): Allelic loss at Drosophila patched gene is highly prevalent in Basal and squamous cell carcinomas of the skin. J Invest Dermatol 126, 1152–1158

Diepgen TL, Mahler V (2002): The epidemiology of skin cancer. Br J Dermatol 146, 1–6

Dierks C, Grbic J, Zirlik K, Beigi R, Englund NP, Guo G-R, Veelken H, Engelhardt M, Mertelsmann R, Kelleher JF, et al. (2007): Essential role of stromally induced hedgehog signaling in B-cell malignancies. Nat Med 13, 944–951

Elmets CA, Cala CM, Xu H (2014): Photoimmunology. Dermatol Clin 32, 277–290

Essid N, Chambard JC, Elgaaïed AB (2018): Induction of epithelial-mesenchymal transition (EMT) and Gli1 expression in head and neck squamous cell carcinoma (HNSCC) spheroid cultures. Bosn J Basic Med Sci 18, 336–346

Euvrard S, Kanitakis J, Claudy A (2003): Skin Cancers after Organ Transplantation. N Engl J Med 348, 1681–1691

Fan L, Pepicelli CV, Dibble CC, Catbagan W, Zarycki JL, Laciak R, Gipp J, Shaw A, Lamm MLG, Munoz A, et al. (2004): Hedgehog signaling promotes prostate xenograft tumor growth. Endocrinology 145, 3961–3970

Feldmann G, Fendrich V, McGovern K, Bedja D, Bisht S, Alvarez H, Koorstra J-BM, Habbe N, Karikari C, Mullendore M, et al. (2008): An orally bioavailable small-molecule inhibitor of Hedgehog signaling inhibits tumor initiation and metastasis in pancreatic cancer. Mol Cancer Ther 7, 2725–2735

Fichter CD, Gudernatsch V, Przypadlo CM, Follo M, Schmidt G, Werner M, Lassmann S (2014): ErbB targeting inhibitors repress cell migration of esophageal squamous cell carcinoma and adenocarcinoma cells by distinct signaling pathways. J Mol Med 92, 1209–1223

Fogarty GB, Conus NM, Chu J, McArthur G (2007): Characterization of the expression and activation of the epidermal growth factor receptor in squamous cell carcinoma of the skin. Br J Dermatol 156, 92–98

Fogarty MP, Emmenegger BA, Grasfeder LL, Oliver TG, Wechsler-Reya RJ (2007): Fibroblast growth factor blocks Sonic hedgehog signaling in neuronal precursors and tumor cells. Proc Natl Acad Sci 104, 2973–2978

Fujiwara T, Eguchi T, Sogawa C, Ono K, Murakami J, Ibaragi S, Asaumi J, Calderwood SK, Okamoto K, Kozaki K (2018): Carcinogenic epithelial-mesenchymal transition initiated by oral cancer exosomes is inhibited by anti-EGFR antibody cetuximab. Oral Oncol 86, 251–257

Garcovich S, Colloca G, Sollena P, Andrea B, Balducci L, Cho WC, Bernabei R, Peris K (2017): Skin Cancer Epidemics in the Elderly as An Emerging Issue in Geriatric Oncology. Aging Dis 8, 643

Gurney B, Newlands C (2014): Management of regional metastatic disease in head and neck cutaneous malignancy. 1. Cutaneous squamous cell carcinoma. Br J Oral Maxillofac Surg 52, 294–300

Hahn H, Wicking C, Zaphiropoulous PG, Gailani MR, Shanley S, Chidambaram A, Vorechovsky I, Holmberg E, Unden AB, Gillies S, et al. (1996): Mutations of the human homolog of Drosophila patched in the nevoid basal cell carcinoma syndrome. Cell 85, 841–851

Hazelbag S, Kenter GG, Gorter A, Dreef EJ, Koopman LA, Violette SM, Weinreb PH, Fleuren GJ (2007): Overexpression of the alpha v beta 6 integrin in cervical squamous cell carcinoma is a prognostic factor for decreased survival. J Pathol 212, 316–324

Heimberger AB, Hlatky R, Suki D, Yang D, Weinberg J, Gilbert M, Sawaya R, Aldape K (2005): Prognostic effect of epidermal growth factor receptor and EGFRvIII in glioblastoma multiforme patients. Clin Cancer Res Off J Am Assoc Cancer Res 11, 1462–1466

Hellemans J, Coucke PJ, Giedion A, De Paepe A, Kramer P, Beemer F, Mortier GR (2003): Homozygous mutations in IHH cause acrocapitofemoral dysplasia, an autosomal recessive disorder with cone-shaped epiphyses in hands and hips. Am J Hum Genet 72, 1040–1046

Herbst RS, Heymach JV, Lippman SM (2008): Lung Cancer. N Engl J Med 359, 1367–1380

Hsu JL, Hung M-C (2016): The role of HER2, EGFR, and other receptor tyrosine kinases in breast cancer. Cancer Metastasis Rev 35, 575–588

Hutchin ME, Kariapper MST, Grachtchouk M, Wang A, Wei L, Cummings D, Liu J, Michael LE, Glick A, Dlugosz AA (2005): Sustained Hedgehog signaling is required for basal cell carcinoma proliferation and survival: conditional skin tumorigenesis recapitulates the hair growth cycle. Genes Dev 19, 214–223

Hynes NE, MacDonald G (2009): ErbB receptors and signaling pathways in cancer. Curr Opin Cell Biol 21, 177–184

Iarrobino A, Messina JL, Kudchadkar R, Sondak VK (2013): Emergence of a squamous cell carcinoma phenotype following treatment of metastatic basal cell carcinoma with vismodegib. J Am Acad Dermatol 69, e33-34

Jacobsen PF, Jenkyn DJ, Papadimitriou JM (1985): Establishment of a human medulloblastoma cell line and its heterotransplantation into nude mice. J Neuropathol Exp Neurol 44, 472–485

Janes SM, Watt FM (2006): New roles for integrins in squamous-cell carcinoma. Nat Rev Cancer 6, 175–183

Jia J, Tong C, Wang B, Luo L, Jiang J (2004): Hedgehog signalling activity of Smoothened requires phosphorylation by protein kinase A and casein kinase I. Nature 432, 1045–1050

Johnson J-LFA, Hall TE, Dyson JM, Sonntag C, Ayers K, Berger S, Gautier P, Mitchell C, Hollway GE, Currie PD (2012): Scube activity is necessary for Hedgehog signal transduction in vivo. Dev Biol 368, 193–202

Jungbluth AA, Stockert E, Huang HJS, Collins VP, Coplan K, Iversen K, Kolb D, Johns TJ, Scott AM, Gullick WJ, et al. (2003): A monoclonal antibody recognizing human cancers with amplification/overexpression of the human epidermal growth factor receptor. Proc Natl Acad Sci U S A 100, 639–644

Kallini JR, Hamed N, Khachemoune A (2015): Squamous cell carcinoma of the skin: epidemiology, classification, management, and novel trends. Int J Dermatol 54, 130–140

Keysar SB, Le PN, Anderson RT, Morton JJ, Bowles DW, Paylor JJ, Vogler BW, Thorburn J, Fernandez P, Glogowska MJ, et al. (2013): Hedgehog Signaling Alters Reliance on EGF Receptor Signaling and Mediates Anti-EGFR Therapeutic Resistance in Head and Neck Cancer. Cancer Res 73, 3381–3392

Kripke ML (1974): Antigenicity of murine skin tumors induced by ultraviolet light. J Natl Cancer Inst 53, 1333–1336

Lauth M, Bergström A, Shimokawa T, Toftgård R (2007): Inhibition of GLI-mediated transcription and tumor cell growth by small-molecule antagonists. Proc Natl Acad Sci U S A 104, 8455–8460

Lichon V, Khachemoune A (2007): Xeroderma pigmentosum: beyond skin cancer. J Drugs Dermatol JDD 6, 281–288

Lim W, Kim H, Ko H (2019): Delphinidin inhibits epidermal growth factor-induced epithelial-to-mesenchymal transition in hepatocellular carcinoma cells. J Cell Biochem 120, 9887–9899

Lindsey S, Langhans SA (2015): Epidermal growth factor signaling in transformed cells. Int Rev Cell Mol Biol 314, 1–41

Logan CY, Nusse R (2004): THE WNT SIGNALING PATHWAY IN DEVELOPMENT AND DISEASE. Annu Rev Cell Dev Biol 20, 781–810

Lomas A, Leonardi-Bee J, Bath-Hextall F (2012): A systematic review of worldwide incidence of nonmelanoma skin cancer. Br J Dermatol 166, 1069–1080

Lowenstein EJ, Daly RJ, Batzer AG, Li W, Margolis B, Lammers R, Ullrich A, Skolnik EY, Bar-Sagi D, Schlessinger J (1992): The SH2 and SH3 domain-containing protein GRB2 links receptor tyrosine kinases to ras signaling. Cell 70, 431–442

Lu J, Liu L, Zheng M, Li X, Wu A, Wu Q, Liao C, Zou J, Song H (2018): MEKK2 and MEKK3 suppress Hedgehog pathway-dependent medulloblastoma by inhibiting GLI1 function. Oncogene 37, 3864–3878

Lum L, Zhang C, Oh S, Mann RK, von Kessler DP, Taipale J, Weis-Garcia F, Gong R, Wang B, Beachy PA (2003): Hedgehog signal transduction via Smoothened association with

a cytoplasmic complex scaffolded by the atypical kinesin, Costal-2. Mol Cell 12, 1261–1274

Ma X, Sheng T, Zhang Y, Zhang X, He J, Huang S, Chen K, Sultz J, Adegboyega PA, Zhang H, Xie J (2006): Hedgehog signaling is activated in subsets of esophageal cancers. Int J Cancer 118, 139–148

Maeda O, Kondo M, Fujita T, Usami N, Fukui T, Shimokata K, Ando T, Goto H, Sekido Y (2006): Enhancement of GLI1-transcriptional activity by beta-catenin in human cancer cells. Oncol Rep 16, 91–96

Mastrangelo E, Milani M (2018): Role and inhibition of GLI1 protein in cancer. Lung Cancer Targets Ther 9, 35–43

Maubec E, Petrow P, Scheer-Senyarich I, Duvillard P, Lacroix L, Gelly J, Certain A, Duval X, Crickx B, Buffard V, et al. (2011): Phase II study of cetuximab as first-line single-drug therapy in patients with unresectable squamous cell carcinoma of the skin. J Clin Oncol Off J Am Soc Clin Oncol 29, 3419–3426

Mauerer A, Herschberger E, Dietmaier W, Landthaler M, Hafner C (2011): Low incidence of EGFR and HRAS mutations in cutaneous squamous cell carcinomas of a German cohort. Exp Dermatol 20, 848–850

Maule M, Scelo G, Pastore G, Brennan P, Hemminki K, Tracey E, Sankila R, Weiderpass E, Olsen JH, McBride ML, et al. (2007): Risk of Second Malignant Neoplasms After Childhood Leukemia and Lymphoma: An International Study. JNCI J Natl Cancer Inst 99, 790–800

Miller SJ (2000): The National Comprehensive Cancer Network (NCCN) guidelines of care for nonmelanoma skin cancers. Dermatol Surg Off Publ Am Soc Dermatol Surg Al 26, 289–292

Mohan SV, Chang J, Li S, Henry AS, Wood DJ, Chang ALS (2016): Increased Risk of Cutaneous Squamous Cell Carcinoma After Vismodegib Therapy for Basal Cell Carcinoma. JAMA Dermatol 152, 527–532

Morris EJ, Jha S, Restaino CR, Dayananth P, Zhu H, Cooper A, Carr D, Deng Y, Jin W, Black S, et al. (2013): Discovery of a Novel ERK Inhibitor with Activity in Models of Acquired Resistance to BRAF and MEK Inhibitors. Cancer Discov 3, 742–750

Moscatello DK, Holgado-Madruga M, Godwin AK, Ramirez G, Gunn G, Zoltick PW, Biegel JA, Hayes RL, Wong AJ (1995): Frequent expression of a mutant epidermal growth factor receptor in multiple human tumors. Cancer Res 55, 5536–5539

Nelson MA, Einspahr JG, Alberts DS, Balfour CA, Wymer JA, Welch KL, Salasche SJ, Bangert JL, Grogan TM, Bozzo PO (1994): Analysis of the p53 gene in human precancerous actinic keratosis lesions and squamous cell cancers. Cancer Lett 85, 23–29

Nicolas M, Wolfer A, Raj K, Kummer JA, Mill P, van Noort M, Hui C, Clevers H, Dotto GP, Radtke F (2003): Notch1 functions as a tumor suppressor in mouse skin. Nat Genet 33, 416–421

Noubissi FK, Goswami S, Sanek NA, Kawakami K, Minamoto T, Moser A, Grinblat Y, Spiegelman VS (2009): Wnt signaling stimulates transcriptional outcome of the Hedgehog pathway by stabilizing GLI1 mRNA. Cancer Res 69, 8572–8578

Noubissi FK, Kim T, Kawahara TN, Aughenbaugh WD, Berg E, Longley BJ, Athar M, Spiegelman VS (2014): Role of CRD-BP in the growth of human basal cell carcinoma cells. J Invest Dermatol 134, 1718–1724

Nüsslein-Volhard C, Wieschaus E (1980): Mutations affecting segment number and polarity in Drosophila. Nature 287, 795–801

Ohlmeyer JT, Kalderon D (1998): Hedgehog stimulates maturation of Cubitus interruptus into a labile transcriptional activator. Nature 396, 749–753

Orouji A, Goerdt S, Utikal J, Leverkus M (2014): Multiple highly and moderately differentiated squamous cell carcinomas of the skin during vismodegib treatment of inoperable basal cell carcinoma. Br J Dermatol 171, 431–433

Pepinsky RB, Zeng C, Wen D, Rayhorn P, Baker DP, Williams KP, Bixler SA, Ambrose CM, Garber EA, Miatkowski K, et al. (1998): Identification of a palmitic acid-modified form of human Sonic hedgehog. J Biol Chem 273, 14037–14045

Petrova R, Joyner AL (2014): Roles for Hedgehog signaling in adult organ homeostasis and repair. Dev Camb Engl 141, 3445–3457

Ping XL, Ratner D, Zhang H, Wu XL, Zhang MJ, Chen FF, Silvers DN, Peacocke M, Tsou HC (2001): PTCH mutations in squamous cell carcinoma of the skin. J Invest Dermatol 116, 614–616

Po A, Silvano M, Miele E, Capalbo C, Eramo A, Salvati V, Todaro M, Besharat ZM, Catanzaro G, Cucchi D, et al. (2017): Noncanonical GLI1 signaling promotes stemness features and in vivo growth in lung adenocarcinoma. Oncogene 36, 4641–4652

Polizio AH, Chinchilla P, Chen X, Kim S, Manning DR, Riobo NA (2011): Heterotrimeric Gi proteins link Hedgehog signaling to activation of Rho small GTPases to promote fibroblast migration. J Biol Chem 286, 19589–19596

Popp S, Waltering S, Boukamp P, Holtgreve-Grez H, Jauch A, Proby C, Leigh IM (2000): Genetic Characterization of a Human Skin Carcinoma Progression Model: from Primary Tumor to Metastasis. J Invest Dermatol 115, 1095–1103

Porter JA, Young KE, Beachy PA (1996): Cholesterol modification of hedgehog signaling proteins in animal development. Science 274, 255–259

Poulalhon N, Dalle S, Balme B, Thomas L (2015): Fast-growing cutaneous squamous cell carcinoma in a patient treated with vismodegib. Dermatol Basel Switz 230, 101–104

Prodromou NV, Thompson CL, Osborn DPS, Cogger KF, Ashworth R, Knight MM, Beales PL, Chapple JP (2012): Heat shock induces rapid resorption of primary cilia. J Cell Sci 125, 4297–4305

Pyczek J (2018): Hedgehog signaling in cutaneous squamous cell carcinoma. PhD thesis Göttingen 2018

Qualtrough D, Buda A, Gaffield W, Williams AC, Paraskeva C (2004): Hedgehog signalling in colorectal tumour cells: induction of apoptosis with cyclopamine treatment. Int J Cancer 110, 831–837

Ra SH, Li X, Binder S (2011): Molecular discrimination of cutaneous squamous cell carcinoma from actinic keratosis and normal skin. Mod Pathol 24, 963–973

Raffel C, Jenkins RB, Frederick L, Hebrink D, Alderete B, Fults DW, James CD (1997): Sporadic medulloblastomas contain PTCH mutations. Cancer Res 57, 842–845

Reinchisi G, Parada M, Lois P, Oyanadel C, Shaughnessy R, Gonzalez A, Palma V (2013): Sonic Hedgehog modulates EGFR dependent proliferation of neural stem cells during late mouse embryogenesis through EGFR transactivation. Front Cell Neurosci 7, 166

Richards SA, Dreisbach VC, Murphy LO, Blenis J (2001): Characterization of regulatory events associated with membrane targeting of p90 ribosomal S6 kinase 1. Mol Cell Biol 21, 7470–7480

Robbins DJ, Fei DL, Riobo NA (2012): The Hedgehog Signal Transduction Network. Sci Signal 5, re6

Roskoski R (2012): ERK1/2 MAP kinases: structure, function, and regulation. Pharmacol Res 66, 105–143

Roskoski R (2014): The ErbB/HER family of protein-tyrosine kinases and cancer. Pharmacol Res 79, 34–74

Rowe DE, Carroll RJ, Day CL (1992): Prognostic factors for local recurrence, metastasis, and survival rates in squamous cell carcinoma of the skin, ear, and lip. Implications for treatment modality selection. J Am Acad Dermatol 26, 976–990

Saintes C, Saint-Jean M, Brocard A, Peuvrel L, Renaut JJ, Khammari A, Quéreux G, Dréno B (2015): Development of squamous cell carcinoma into basal cell carcinoma under treatment with Vismodegib. J Eur Acad Dermatol Venereol JEADV 29, 1006–1009

Salasche SJ (2000): Epidemiology of actinic keratoses and squamous cell carcinoma. J Am Acad Dermatol 42, S4–S7

Scales SJ, de Sauvage FJ (2009): Mechanisms of Hedgehog pathway activation in cancer and implications for therapy. Trends Pharmacol Sci 30, 303–312

Schaeffer D, Somarelli JA, Hanna G, Palmer GM, Garcia-Blanco MA (2014): Cellular Migration and Invasion Uncoupled: Increased Migration Is Not an Inexorable Consequence of Epithelial-to-Mesenchymal Transition. Mol Cell Biol 34, 3486–3499

Schmults CD, Karia PS, Carter JB, Han J, Qureshi AA (2013): Factors Predictive of Recurrence and Death From Cutaneous Squamous Cell Carcinoma: A 10-Year, Single-Institution Cohort Study. JAMA Dermatol 149, 541

Schnidar H, Eberl M, Klingler S, Mangelberger D, Kasper M, Hauser-Kronberger C, Regl G, Kroismayr R, Moriggl R, Sibilia M, Aberger F (2009): Epidermal growth factor receptor signaling synergizes with Hedgehog/GLI in oncogenic transformation via activation of the MEK/ERK/JUN pathway. Cancer Res 69, 1284–1292

Shimizu T, Izumi H, Oga A, Furumoto H, Murakami T, Ofuji R, Muto M, Sasaki K (2001): Epidermal growth factor receptor overexpression and genetic aberrations in metastatic squamous-cell carcinoma of the skin. Dermatol Basel Switz 202, 203–206

Singh R, Dhanyamraju PK, Lauth M (2017): DYRK1B blocks canonical and promotes non-canonical Hedgehog signaling through activation of the mTOR/AKT pathway. Oncotarget 8, 833–845

Song L, Li Z-Y, Liu W-P, Zhao M-R (2015): Crosstalk between Wnt/β-catenin and Hedgehog/Gli signaling pathways in colon cancer and implications for therapy. Cancer Biol Ther 16, 1–7

Spindler K-LG, Olsen DA, Nielsen JN, Brandslund I, Poulsen HS, Villingshøj M, Jakobsen A (2006): Lack of the type III epidermal growth factor receptor mutation in colorectal cancer. Anticancer Res 26, 4889–4893

Staples MP, Elwood M, Burton RC, Williams JL, Marks R, Giles GG (2006): Non-melanoma skin cancer in Australia: the 2002 national survey and trends since 1985. Med J Aust 184, 6–10

Stecca B, Mas C, Clement V, Zbinden M, Correa R, Piguet V, Beermann F, Ruiz I Altaba A (2007): Melanomas require HEDGEHOG-GLI signaling regulated by interactions between GLI1 and the RAS-MEK/AKT pathways. Proc Natl Acad Sci U S A 104, 5895–5900

Steffensen KD, Waldstrøm M, Olsen DA, Corydon T, Lorentzen KA, Knudsen HJ, Jeppesen U, Brandslund I, Jakobsen A (2008): Mutant epidermal growth factor receptor in benign, borderline, and malignant ovarian tumors. Clin Cancer Res Off J Am Assoc Cancer Res 14, 3278–3282

Stern RS (2012): The risk of squamous cell and basal cell cancer associated with psoralen and ultraviolet A therapy: A 30-year prospective study. J Am Acad Dermatol 66, 553–562

St-Jacques B, Hammerschmidt M, McMahon AP (1999): Indian hedgehog signaling regulates proliferation and differentiation of chondrocytes and is essential for bone formation. Genes Dev 13, 2072–2086

Tanese K, Emoto K, Kubota N, Fukuma M, Sakamoto M (2018): Immunohistochemical visualization of the signature of activated Hedgehog signaling pathway in cutaneous epithelial tumors. J Dermatol

Tang Z, Dai S, He Y, Doty RA, Shultz LD, Sampson SB, Dai C (2015): MEK Guards Proteome Stability and Inhibits Tumor-Suppressive Amyloidogenesis via HSF1. Cell 160, 729–744

Taylor MD, Liu L, Raffel C, Hui C, Mainprize TG, Zhang X, Agatep R, Chiappa S, Gao L, Lowrance A, et al. (2002): Mutations in SUFU predispose to medulloblastoma. Nat Genet 31, 306–310

Thayer SP, di Magliano MP, Heiser PW, Nielsen CM, Roberts DJ, Lauwers GY, Qi YP, Gysin S, Fernández-del Castillo C, Yajnik V, et al. (2003): Hedgehog is an early and late mediator of pancreatic cancer tumorigenesis. Nature 425, 851–856

Thibert C, Teillet M-A, Lapointe F, Mazelin L, Le Douarin NM, Mehlen P (2003): Inhibition of neuroepithelial patched-induced apoptosis by sonic hedgehog. Science 301, 843–846

Toll A, Salgado R, Yébenes M, Martín-Ezquerra G, Gilaberte M, Baró T, Solé F, Alameda F, Espinet B, Pujol RM (2010): Epidermal growth factor receptor gene numerical aberrations are frequent events in actinic keratoses and invasive cutaneous squamous cell carcinomas. Exp Dermatol 19, 151–153

Tostar U, Malm CJ, Meis-Kindblom JM, Kindblom L-G, Toftgård R, Undén AB (2006): Deregulation of the hedgehog signalling pathway: a possible role for the PTCH and SUFU genes in human rhabdomyoma and rhabdomyosarcoma development. J Pathol 208, 17–25

Traiffort E, Dubourg C, Faure H, Rognan D, Odent S, Durou M-R, David V, Ruat M (2004): Functional characterization of sonic hedgehog mutations associated with holoprosencephaly. J Biol Chem 279, 42889–42897

Uhlenhake E (2013): Optimal treatment of actinic keratoses. Clin Interv Aging 29

Ullrich A, Coussens L, Hayflick JS, Dull TJ, Gray A, Tam AW, Lee J, Yarden Y, Libermann TA, Schlessinger J (1984): Human epidermal growth factor receptor cDNA sequence and aberrant expression of the amplified gene in A431 epidermoid carcinoma cells. Nature 309, 418–425

Ushiro H, Cohen S (1980): Identification of phosphotyrosine as a product of epidermal growth factor-activated protein kinase in A-431 cell membranes. J Biol Chem 255, 8363–8365

Wang Y, Ding Q, Yen C-J, Xia W, Izzo JG, Lang J-Y, Li C-W, Hsu JL, Miller SA, Wang X, et al. (2012): The crosstalk of mTOR/S6K1 and Hedgehog pathways. Cancer Cell 21, 374–387

Wang Y, Jin G, Li Q, Wang Z, Hu W, Li P, Li S, Wu H, Kong X, Gao J, Li Z (2016): Hedgehog Signaling Non-Canonical Activated by Pro-Inflammatory Cytokines in Pancreatic Ductal Adenocarcinoma. J Cancer 7, 2067–2076

Wang Y-F, Yang H-Y, Shi X-Q, Wang Y (2018): Upregulation of microRNA-129-5p inhibits cell invasion, migration and tumor angiogenesis by inhibiting ZIC2 via downregulation of the Hedgehog signaling pathway in cervical cancer. Cancer Biol Ther 19, 1162–1173

Wang Z (2017): ErbB Receptors and Cancer. Methods Mol Biol Clifton NJ 1652, 3–35

Wee P, Wang Z (2017): Epidermal Growth Factor Receptor Cell Proliferation Signaling Pathways. Cancers 9, 52

Weichselbaum RR, Dunphy EJ, Beckett MA, Tybor AG, Moran WJ, Goldman ME, Vokes EE, Panje WR (1989): Epidermal growth factor receptor gene amplification and expression in head and neck cancer cell lines. Head Neck 11, 437–442

Weissenborn SJ, Nindl I, Purdie K, Harwood C, Proby C, Breuer J, Majewski S, Pfister H, Wieland U (2005): Human Papillomavirus-DNA Loads in Actinic Keratoses Exceed those in Non-Melanoma Skin Cancers. J Invest Dermatol 125, 93–97

Whisenant TC, Ho DT, Benz RW, Rogers JS, Kaake RM, Gordon EA, Huang L, Baldi P, Bardwell L (2010): Computational Prediction and Experimental Verification of New MAP Kinase Docking Sites and Substrates Including Gli Transcription Factors. PLoS Comput Biol 6

Xiang X, Zang M, Waelde CA, Wen R, Luo Z (2002): Phosphorylation of 338SSYY341 regulates specific interaction between Raf-1 and MEK1. J Biol Chem 277, 44996–45003

Yang B, Miao S, Li Y (2018): SCUBE2 inhibits the proliferation, migration and invasion of human non-small cell lung cancer cells through regulation of the sonic hedgehog signaling pathway. Gene 672, 143–149

Yao S, Lum L, Beachy P (2006): The ihog cell-surface proteins bind Hedgehog and mediate pathway activation. Cell 125, 343–357

Yauch RL, Gould SE, Scales SJ, Tang T, Tian H, Ahn CP, Marshall D, Fu L, Januario T, Kallop D, et al. (2008): A paracrine requirement for hedgehog signalling in cancer. Nature 455, 406–410

Yu Q, Li D, Wang D, Hu C-M, Sun Y, Tang Y, Shi G (2018): Effect of RAB31 silencing on osteosarcoma cell proliferation and migration through the Hedgehog signaling pathway. J Bone Miner Metab

Yuan Z, Goetz JA, Singh S, Ogden SK, Petty WJ, Black CC, Memoli VA, Dmitrovsky E, Robbins DJ (2007): Frequent requirement of hedgehog signaling in non-small cell lung carcinoma. Oncogene 26, 1046–1055

Zhang R, Wu J, Ferrandon S, Glowacki KJ, Houghton JA (2016): Targeting GLI by GANT61 involves mechanisms dependent on inhibition of both transcription and DNA licensing. Oncotarget 7

Zhang X, Wu L, Xiao T, Tang L, Jia X, Guo Y, Zhang J, Li J, He Y, Su J, et al. (2018): TRAF6 regulates EGF-induced cell transformation and cSCC malignant phenotype through CD147/EGFR. Oncogenesis 7

Zhou J, Zhu G, Huang J, Li L, Du Y, Gao Y, Wu D, Wang X, Hsieh J-T, He D, Wu K (2016): Non-canonical GLI1/2 activation by PI3K/AKT signaling in renal cell carcinoma: A novel potential therapeutic target. Cancer Lett 370, 313–323

Zhou J, Zhao T, Ma L, Liang M, Guo Y-J, Zhao L-M (2017): Cucurbitacin B and SCH772984 exhibit synergistic anti-pancreatic cancer activities by suppressing EGFR, PI3K/Akt/mTOR, STAT3 and ERK signaling. Oncotarget 8

Zhu J, Sun Y, Lu Y, Jiang X, Ma B, Yu L, Zhang J, Dong X, Zhang Q (2018): Glaucocalyxin A exerts anticancer effect on osteosarcoma by inhibiting GLI1 nuclear translocation via regulating PI3K/Akt pathway. Cell Death Dis 9, 708

Zinke J, Schneider FT, Harter PN, Thom S, Ziegler N, Toftgård R, Plate KH, Liebner S (2015): β-Catenin-Gli1 interaction regulates proliferation and tumor growth in medulloblastoma. Mol Cancer 14, 17

Acknowledgments

First of all, I want to express my deep gratitude to my supervisor Prof. Dr. Heidi Hahn, who gave me the opportunity to work on this project and always motivated me by her inspiring ideas. Then I want to thank Dr. Joanna Pyczek for her guidance in the lab and in the project. I would also like to thank Prof. Dr. Michael Schön for his comments and suggestions and for creating a great atmosphere during my thesis committee meetings.

Many thanks go to the lab members: Dr. Julia Dräger, Dr. Nathalia Geyer, Dr. Julia Bauer, Dr. Anja Uhmann, Dr. Frauke Nitzki, Dominik Botermann, Ina Heß, and Anke Frommhold.

I want to thank the Jacob Henle Program for Experimental Medicine for the scholarship, which gave me the opportunity to fully focus on my work in the lab.

Finally, I want to thank my family and friends, who tried their best to support and encourage me.